UNCLASSIFIED

NATIONAL AERONAUTICS AND SPACE ADMINISTRATION

Space Programs Summary 37-46, Vol. II

The Planetary–Interplanetary Program

For the Period May 1 to June 30, 1967

(Title Unclassified)

Classification Changed
UNCLASSIFIED
JPL - Letter to Authority NASA - Langley
dtd Nov. 4 1970, signed by W. E Hanon
Date: Jan. 4, 1971 By: A. Chastain

JET PROPULSION LABORATORY
LIBRARY
OCT 3 1967

Copy No. 435

CALIFORNIA INSTITUTE OF TECHNOLOGY

LAB-D01982

JET PROPULSION LABORATORY
CALIFORNIA INSTITUTE OF TECHNOLOGY
PASADENA, CALIFORNIA

July 31, 1967

UNCLASSIFIED

166123

UNCLASSIFIED

SPACE PROGRAMS SUMMARY 37-46, VOL. II

Copyright © 1967
Jet Propulsion Laboratory
California Institute of Technology

Prepared Under Contract No. NAS 7-100
National Aeronautics and Space Administration

This document contains information affecting the national defense of the United States, within the meaning of the Espionage Laws, Title 18, U.S.C., Sections 793 and 794, the transmission or revelation of which in any manner to an unauthorized person is prohibited by law.

Downgraded at 3 year intervals; declassified after 12 years.

UNCLASSIFIED

UNCLASSIFIED
CONFIDENTIAL

Preface

The Space Programs Summary is a six-volume bimonthly publication designed to report on JPL space exploration programs and related supporting research and advanced development projects. The titles of all volumes of the Space Programs Summary are:

Vol. I. *The Lunar Program* (Confidential)
Vol. II. *The Planetary–Interplanetary Program* (Confidential)
Vol. III. *The Deep Space Network* (Unclassified)
Vol. IV. *Supporting Research and Advanced Development* (Unclassified)
Vol. V. *Supporting Research and Advanced Development* (Confidential)
Vol. VI. *Space Exploration Programs and Space Sciences* (Unclassified)

The Space Programs Summary, Vol. VI, consists of an unclassified digest of appropriate material from Vols. I, II, and III; an original presentation of the JPL quality assurance and reliability efforts, and the environmental- and dynamic-testing facility-development activities; and a reprint of the space science instrumentation studies of Vols. I and II.

Approved by:

W. H. Pickering, *Director*
Jet Propulsion Laboratory

UNCLASSIFIED
CONFIDENTIAL

UNCLASSIFIED
CONFIDENTIAL

Contents

I. *Mariner IV* Project 1
A. Introduction 1

II. *Mariner* Venus 67 Project 2
A. Introduction 2
B. Systems 3
C. Guidance and Control 5

III. *Mariner* Mars 1969 Project 6
A. Introduction 6
B. Project Engineering 7
C. Guidance and Control 16
D. Engineering Mechanics 29

IV. *Voyager* Project 45
A. Introduction 45
B. Telecommunications 46

V. Future Projects 49

UNCLASSIFIED
CONFIDENTIAL

UNCLASSIFIED

I. *Mariner IV* Project

A. Introduction

The *Mariner IV* Project is under the administrative cognizance of the *Mariner* 1967 Project Office, which also directs the *Mariner* Venus 67 Project and the residual activity of the *Mariner* Mars 1964 Project. Residual activity of the *Mariner* Mars 1964 Project consists primarily of continuing analysis of tracking data, publication of results by the principal investigators, and preparation of final reports. However, periodic detection, recording, and commanding activities involving the *Mariner IV* spacecraft have been assigned to the Deep Space Network. Elements of the experimental facilities at Goldstone Station (Venus and Mars Deep Space Stations) have been used to communicate successfully with the spacecraft. The DSN results will be published periodically in Vol. III of future Space Programs Summaries. *Mariner* Venus 67 Project activities are reported in the following Section II.

The objectives, authorized in December 1965, simultaneously with those for the Venus flight, have been established as:

> *The primary objective of the Mariner IV Project is to obtain scientific information on the interplanetary environment in a region of space further from the sun than the orbit of earth during a period of increasing solar activity in 1967, using the Mariner IV spacecraft still operating in orbit around the sun.*
>
> *The secondary objectives are to obtain additional engineering knowledge about the consequences of extended exposure of spacecraft equipment in the interplanetary space environment and to acquire experience in the operation of a planetary spacecraft after a prolonged lifetime in deep space.*

During the May–June reporting period, spacecraft conditioning and data retrieval activities were resumed after Mars Deep Space Station was returned to service.

Three commands (QC-1-1, DC-13 and DC-15) were accepted by the spacecraft, and the Canopus sensor cone angle was then reset to a final angle of 77.9 deg by executing five update steps (DC-17). The roll-limit cycle of the spacecraft is very regular, indicating that the spacecraft is locked onto a well defined signal source. The identity of the star remains unknown because of a lack of data at this time.

Telemetry data were recorded in analog form by Johannesburg Deep Space Station to determine the feasibility of using this station for the continued tracking of *Mariner IV*. Data quality has not been determined, however, because the tapes have not as yet been processed.

An analysis of the engineering telemetry indicates that the spacecraft was subjected to a power transient that resulted in the loss of the traveling-wave-tube transmitter. Since the system is designed to switch radio power amplifiers automatically, it is assumed that the traveling wave tube has failed.

CONFIDENTIAL UNCLASSIFIED

UNCLASSIFIED

II. *Mariner* Venus 67 Project

A. Introduction

The *Mariner* Venus 67 Project is under the administrative cognizance of the *Mariner* 1967 Project Office, which is also responsible for the *Mariner* Mars 1964 Project and the *Mariner IV* Project (see Section I).

1. *Mariner* Venus 67 Project

The major task of the *Mariner* 1967 Project is the Venus flyby mission, named the *Mariner* Venus 67 Project. The following mission objectives have been established:

> *The primary objective of the Mariner Venus 67 Project is to conduct a flyby mission to Venus in 1967 in order to obtain scientific information which will complement and extend the results obtained by Mariner II relevant to determining the origin and nature of Venus and its environment.*
>
> *Secondary objectives are to acquire engineering experience in converting and operating a spacecraft designed for flight to Mars into one flown to Venus, and to obtain information on the interplanetary environment during a period of increasing solar activity.*

With the authorizing of this project late in December 1965, and the launch opportunity occurring in June 1967, the period available to the *Mariner* Venus 67 Project for planning, design, test, and other flight preparation was 18 mo.

The single flight spacecraft, designated M67-2, was prepared by converting the spare spacecraft (MC-4) that was built for the *Mariner* Mars 1964 Project. An *Atlas-Agena D* launch vehicle was used to inject the spacecraft into a 127-day transit trajectory.

Seven scientific experiments were approved for the *Mariner* Venus 67 mission:

Experiment	Principal investigator
S-band radio occultation	Arvydas J. Kliore, Jet Propulsion Laboratory
Ultraviolet photometer	Charles A. Barth, University of Colorado
Dual-frequency radio propagation	Von R. Eshleman, Stanford University
Helium magnetometer	Edward J. Smith, Jet Propulsion Laboratory
Solar plasma	Herbert S. Bridge, Massachusetts Institute of Technology
Trapped radiation	James A. Van Allen, State University of Iowa
Celestial mechanics	John D. Anderson, Jet Propulsion Laboratory

UNCLASSIFIED CONFIDENTIAL

UNCLASSIFIED

The first experiment requires the use of only the RF transmission subsystem on the spacecraft, and the last one utilizes only the tracking doppler data received from the RF carrier. Of the remaining five experiments, four are to be accomplished with the existing instrumentation, with only minor modifications. Only the dual-frequency radio propagation experiment of Stanford University requires the incorporation of a new scientific instrument into the payload.

Other changes to the basic spacecraft design were necessitated by the fact that the spacecraft will travel toward, rather than away from, the sun and also because conversions must be made to accommodate revised encounter sequencing and science payload. In particular, modifications were needed in the following areas:

(1) Scientific data automation system

(2) Antenna pattern and orientation

(3) Thermal control

(4) Solar panel configuration

(5) Planetary sensors

2. *Mariner V*

Mariner V was successfully launched from the AFETR at 02:01 EDT June 14, 1967.

During the normal roll-search mode of the spacecraft, the Canopus sensor locked on the far limb of the earth. Two roll override commands (DC-V21) were then sent to the spacecraft. These commands stepped the spacecraft from the far limb to the near limb of earth and then to the star Canopus.

Prior to the acquisition of Canopus, the science instruments made measurements of the environment in three distinct regions:

(1) Inside the magnetosphere, the trapped radiation detector monitored the Van Allen radiation belts, the helium magnetometer measured the geomagnetic field, and the plasma probe detected no plasma.

(2) Passage through the magnetopause (outer boundary of the magnetosphere) was marked by the first detection of plasma. In this transition region, the plasma probe measured the solar plasma as modified by the passage through the shock wave.

(3) Passage through the plasma shock wave was indicated by a sudden decrease in the magnetic field, and a change in the energy spectrum of the solar plasma to one typical of the interplanetary wind. Disturbances observed in the magnetic field indicated some solar activity. The geiger counter pointed toward the sun detected at least one burst of solar X-rays.

Throughout the period when the spacecraft was rolling, the ultraviolet photometer periodically observed the hydrogen in the earth's geocorona.

The *Mariner V* spacecraft successfully performed a midcourse correction maneuver on June 19, 5 days after launch from Cape Kennedy. Motor burn during the midcourse correction lasted for 17.66 s. As a result of the midcourse correction maneuver, the spacecraft will now pass on the antisolar side of Venus at a distance of 2460 mi from the surface of the planet. The flyby geometry is considered to be well within the tolerance required to meet the mission objectives.

Following the midcourse correction maneuver, ranging instrumentation was turned on for the first time with a *Mariner*-type spacecraft. Ranging data were obtained by the MK-I (lunar) equipment at Pioneer Station and Robledo Station. The MK-II (planetary) ranging equipment at Mars Station also acquired data during a portion of one pass. The ranging data thus far obtained on the *Mariner V* mission exceed that required to determine the trajectory and flyby conditions of the spacecraft. These data are, however, being retained for post-mission analysis to determine the subtle effects not possible to measure with present analytic tools.

The M67-1 flight-support spacecraft has been returned from the AFETR and is now in operation in the Spacecraft Assembly Facility area. This spacecraft will be used to determine the cause of anomalies that may be encountered during flight and to support tests of command operations.

B. Systems

1. Systems-Test-Complex Data System

The systems-test-complex data system (STCDS) computer system was assembled and checked out at AFETR by April 27, and subsequently was connected to the associated data input subsystem located on the STC to enable

UNCLASSIFIED

support of the system verification test May 1. At this time a minor problem appeared in the program logic associated with the duplex TTY machine associated with control of STCDS printouts by the test director. This was promptly fixed by the programmers. During system verification, there was a recurrence of an apparently intermittent failure in one of the eight signal amplifiers in the high-speed analog system used in the autopilot test. This amplifier, which handles the pitch gyro signal, was removed, replaced by a spare, and sent to Astrodata for test and evaluation. No failures were evidenced during this test, which included 12 h of operation at 160°F ambient temperature, and the cause of failure has not yet been determined.

The system verification test, using the M67-1 spacecraft, was followed immediately by system tests of the M67-2 spacecraft. During this period it was evident that the computer system air conditioning at Bldg AO was inadequate to keep the computer system temperatures below the alarm levels, and modifications to the air distribution were made. Computer malfunctions necessitated an adjustment at this time, which may have been associated with either the over-temperature condition or with transportation of the system from JPL. From this time on, only minor problems occurred, and the M67-1 spacecraft system tests starting May 12, as well as other tests and investigations involving either spacecraft, were fully supported. The STCDS supported 231 h of real-time testing and 63 h of nonreal-time testing at AFETR. The total downtime for the computer system was 1.8 h, of which 1.1 h were caused by air conditioning problems, power failures, and fire in a circuit breaker box. The total uptime, or computer system availability, was 99.4% even though the above-mentioned failures are considered as downtime. Development was continued on the program used for nonreal-time analysis of data recorded during previous system tests. This program proved valuable for recovering and evaluating Canopus sensor data in connection with the investigation of noisy sensor output during the Cape Kennedy Deep Space Station/spacecraft interface test. The system supported launch countdowns and approximately 12 min of launch phase operation of the spacecraft while telemetry data were being received over the *Agena* link via Bldg. AE or from Antigua via Bldg. AO.

The STCDS was retained at AFETR to support any testing on the M67-1 spacecraft through first midcourse maneuver, and was disassembled June 20 for return to JPL for reinstallation in the Spacecraft Assembly Facility June 30. The system will be used for program development for *Mariner* Mars 1969, and will continue to be available for M67-1 spacecraft test support as required.

The general functional requirements of the STCDS were established in the February–July 1966 period by discussions with the Systems Test and Operations Section. These requirements were based on experience with the *Mariner* Mars 1964 computer data system and enabled the STCDS programmers to begin planning the programming and buffer structures for data acquisition and recording, the decommutation routines for telemetry data, and the output processors for the line printer and TTY printers located on the systems test complex. The standard processing requirements for telemetry and analog data, and for events and status data were well understood functionally since they were a carryover from the *Mariner* Mars 1964 system, and needed only to be adapted for use in the CDC 3300 computer system before coding.

Subsequently, all special processing and additional requirements for processing the acquired data in real time or nonreal time were defined by a series of user service requests (USRs) which were approved by the Systems Test and Operations manager prior to implementation by the STCDS programming and hardware cognizant engineers. The most significant USRs were those for science DAS data acquisition, data recording, and processing for display on a separate STCDS line printer, as described in SPS 37-42, Vol. II (Confidential).

A total of 35 USRs was approved, of which 11 could not be implemented or were only partially implemented. The reasons for this deficiency were partly STCDS hardware problems, including the lack of a functioning low-speed analog system, as reported in SPS 37-45, Vol. II (Confidential), the lack of a proper interface with the RF counter in the radio subsystem operational support equipment (OSE), and inability to input the CC&S OSE 1 pulse/s clock pulse to the computer system via an external interrupt channel. The inability to accommodate a real-time plot program in the computer because of core size limitations (SPS 37-44, Vol. II, Confidential) prevented full implementation of several USRs. Also, improper operation of the attitude control jet pressure transducers prevented the computer system from acquiring the data necessary to satisfy several additional USRs.

It is anticipated that the STCDS will be operational in the JPL Spacecraft Assembly Facility by July 7, with the computer system located in an enlarged area designed to

UNCLASSIFIED

accommodate the additional equipment to be used to support *Mariner* Mars 1969 spacecraft systems testing.

C. Guidance and Control

1. Attitude Control Subsystem

The AFETR testing phase on the *Mariner* Venus 67 spacecraft started May 2, 1967 and proceeded until launch, June 14, 1967 at 06:01 GMT; two problems within the attitude control subsystem arose, both related to the Canopus sensor. On May 9, 1967, near the conclusion of the DSIF compatibility test, the flight Canopus sensor was noted to have a varying intensity output, from "dark" to about 1/15 × Canopus, with no light input. Since the OSE hood was still attached to the sensor, the possibility of a light leak through the hood–sensor mechanical interface was investigated first; no such leak was apparent. The flight spare sensor was examined and it displayed the same type of noise; the flight sensor was then removed from the spacecraft and taken to the laboratory where the noisy output was again obtained. It was decided to run the sensor for a continuous 24-h period, recording the output of the intensity and roll error channels. Approximately 6 h after this test started, the noise disappeared, and did not recur. When the flight spare sensor was turned on, it also was quiet.

It was recognized then that the noise seen would probably not be discernible in flight, since the lowest intensity seen by the *Mariner* Mars 1964 sensor was above this level of noise. However, since the cause of the noise was unknown, further investigation was indicated. The flight sensor was accordingly replaced on the flight spacecraft to participate in further testing, and the flight spare sensor was returned to JPL for evaluation of its electromagnetic-interference sensitive properties. The prototype sensor was sent to AFETR to replace the flight spare sensor on the flight spare spacecraft for further testing, until such time as it could be returned to AFETR.

The results of the electromagnetic-interference tests at Pasadena could not attribute the cause of the observed noise to interference. There appeared to be several bands of frequencies and several discrete frequencies to which the sensor responded (in a range from 50 MHz to 10 GHz) but the power required to produce the noise observed at AFETR was high, on the order of 0.1 to 1 w/m^2. To date, the cause of the noise is still unknown; however, the symptoms have never reappeared on either sensor. Some alternative lines of investigation are being pursued (e.g., radiation effects) but, as suspected, the background light on the sensor currently in flight has been above the level of the noise and thus a recurrence on the flight sensor would not be detectable.

The second problem experienced was with the prototype sensor that replaced the flight spare sensor for a period of a week during the AFETR testing. During cycling of the Canopus sensor cone angle ring counter, a relay in the ring counter "hung up" (i.e., one set of contacts did not transfer completely), rendering the ring counter circuit inoperative. This condition had been observed before, and could be compensated for by careful selection of relays. Since this had already been accomplished for the flight sensor (but not for the flight spare unit), no action was taken.

As stated, M67-1 (now *Mariner V*) was launched June 14. Since then, during sun acquisition, magnetometer calibration, Canopus acquisition, and midcourse maneuver, the attitude control subsystem has performed with no anomalies.

UNCLASSIFIED

UNCLASSIFIED

III. *Mariner* Mars 1969 Project

A. Introduction

The *Mariner* Mars 1969 Project was initiated in late-December 1965 and formally tasked on February 1, 1966. The primary objective is to conduct two Mars flyby missions in 1969 to make exploratory investigations of the planet which will set the basis for future experiments—particularly those relevant to the search for extraterrestrial life. The secondary objective is to develop the technology needed for succeeding Mars missions.

The spacecraft design concept will be based on the configuration of the successful *Mariner IV* spacecraft, with considerable modifications to meet the 1969 mission requirements and to enhance mission reliability.

The launch vehicle will be the *Atlas/Centaur* SLV-3C. This vehicle, developed under contract for and direction by the Lewis Research Center by General Dynamics/Convair, has a single- or double-burn capability in its second stage and a considerably increased performance rating over the *Atlas D/Agena D* used in the *Mariner IV* mission.

Mariner Mars 1969 missions will be supported by the Eastern Test Range launch facilities at Cape Kennedy, the tracking and data acquisition facilities of the Deep Space Network, and other NASA facilities.

Six planetary-science experiments have been selected by NASA for the *Mariner* Mars 1969 missions; they are listed in Table 1. Additionally, a planetary-approach-guidance engineering experiment will be incorporated to test the feasibility and flight-readiness of on-board optical sensors and associated data processing techniques necessary for optical approach guidance.

The launch period available for 1969 Mars launches, using planar and dog-leg direct-ascent trajectories, runs from the middle of February to the beginning of April. Arrival is planned to occur between August 1 and 10, 1969; two separate aiming points will be chosen.

During this reporting period, the Project continued to refine its design elements; spacecraft subsystem efforts were directed toward manufacturing procurements. The Mission Requirements portion of the Mission Plan and Requirements was approved and released; the Mission Plan portion is expected to be released within the next few months. Interface documents for Spacecraft/Mission Operations System and Spacecraft/DSIF telecommunica-

UNCLASSIFIED

UNCLASSIFIED

Table 1. *Mariner* Mars 1969 scientific investigations

Experiment	Scientific investigator	Affiliation
Television	R. B. Leighton[a]	California Institute of Technology (CIT)
	B. C. Murray	CIT
	R. P. Sharp	CIT
	N. H. Horowitz	CIT
	J. D. Allen	Jet Propulsion Laboratory (JPL)
	A. G. Herriman	JPL
	R. K. Sloan	JPL
	L. R. Malling	Massachusetts Institute of Technology
	M. E. Davies	Rand Corporation
	C. Leovy	Rand Corporation
Infrared spectrometer	G. C. Pimentel[a]	University of California, Berkeley (UCB)
	K. C. Herr	UCB
Ultraviolet airglow spectrometer	C. A. Barth[a]	University of Colorado
	W. G. Fastie	Johns Hopkins University
Infrared radiometer	G. Neugebauer[a]	CIT
	G. Munch	CIT
	S. C. Chase	Santa Barbara Research Center
S-band occultation	A. J. Kliore[a]	JPL
	D. L. Cain	JPL
	G. S. Levy	JPL
Celestial mechanics	J. D. Anderson[a]	JPL

[a] Principal investigator.

tions were prepared and reviewed; these will be issued in July 1967. The fifth quarterly project review was conducted in conjunction with an experimenter's meeting on June 27 and 28, 1967.

The spacecraft design underwent minor changes during the period, as described in B. Project Engineering, which follows. In addition, revision of the Spacecraft Design Book was undertaken to reflect the various changes accomplished since, and as a result of, the Preliminary Design Review of November 1966. Of the 16 Phase II-type subcontracts for spacecraft subsystem fabrication, RFPs were issued on 12 and proposals received on 8 (one Phase II subcontract had been issued previously).

The Mission Operations Design Book, the functional requirements portion of the Software System Design Book, and a preliminary Space Flight Operations Plan were completed during the reporting period. A functional design review of the mission operations and tracking and data acquisition systems is scheduled for July 6 and 7, 1967.

B. Project Engineering

1. Spacecraft Design

Numerous changes have been made to the *Mariner* Mars 1969 spacecraft design during the reporting period. The principal changes and the reasons for them are listed in Table 2 and discussed in subsequent paragraphs.

The solar panel support structure has been strengthened to support the added weight of the 20-mil solar panel cover glass.

The structures subsystem was given the responsibility for three accelerometer amplifiers, which formerly were the responsibility of the flight telemetry subsystem.

The total power consumption of the radio frequency subsystem has increased from 70 to 92.3 W in the low-power mode and from 105 to 131.3 W in the high-power mode. This was due to increases in the original estimates of the power requirements of the traveling wave tube power amplifiers and the exciters.

For purposes of redundancy, additional interface circuitry was added between the flight command subsystem and the central computer and sequencer (CC&S) to provide two separate paths for coded commands to reach the CC&S. One path leads to the fixed sequencer and the other leads to the computer.

The 6-mil solar panel cover glass was replaced with 20-mil cover glass in order to provide more protection against solar panel solar flare damage. This incorporation adds approximately 25 W to the capability of the solar panels in the case of maximum solar flare damage.

A fuse box was added to the power subsystem to house the fuses for the spacecraft's temperature control heaters. Location of the fuses at the power source provides the maximum fusing protection by protecting against shorts in the cabling as well as in the heaters. It also provides a single access for heater fuse inspection and replacement during system test and launch operations.

A new command, *heater power switch* was incorporated. This new command toggles the dc thermostatic heaters which are under the science platform thermal blanket between the dc bus and the battery. It provides the capability to improve the solar panel power margin during encounter, if circumstances dictate. It also provides a means for inflight checks on the condition of the battery.

UNCLASSIFIED

Table 2. Recent changes to spacecraft design

Subsystem	Change
Structures	Strengthening of solar panel support structure
	Additional accelerometer amplifiers
Radio frequency	Power consumption increase
Flight command	Redundant coded command interfaces
Power	20-mil cover glass incorporation
	Addition of fuse box
	Incorporation of DC-50, heater power switch
	Data storage subsystem power switching change
	Voltage fail-sense circuitry change
Central computer and sequencer	No significant changes
Flight telemetry	Incorporation of independent mode change capability
Attitude control	Reduction in pitch and yaw deadband
Pyrotechnic	Deletion of ultraviolet spectrometer cover removal function
	Change in infrared spectrometer motor start/cooldown mechanization
Cabling	No significant changes
Propulsion	Rocket engine relocation
Temperature control	Deletion of promethium 147 heat sources
Mechanical devices	Incorporation of pneumatic latch for scan platform
Approach guidance	No significant changes
Data storage	Deletion of analog/digital transfer wait-state
	Deletion of recording turnoff from lack of data automation subsystem sync
Data automation	Addition of backup command to start recorder
Scan control	Scan position telemetry
Ultraviolet spectrometer	Elimination of ultraviolet spectrometer cover
Television	Incorporation of signal to time analog tape recorder
	Implementation of TV cover removal, DC-46
	Addition of TV preconditioning command, DC-48
	Incorporation of capability to reset TV aperture
Infrared spectrometer	Choice of hydrogen for infrared spectrometer coolant gas
Infrared radiometer	Addition of precondition command, DC-48

Circuitry was added to turn on the data storage subsystem power upon receipt of CC&S command *P1*. This incorporation formed a part of the means used to remedy a spurious command problem which existed between the data automation subsystem and the data storage subsystem.

The voltage fail-sense circuitry in the power subsystem was moved from the output of the 2400-Hz inverter to the output of the booster regulator. This change improved the capability of the fail-sense circuitry to sense out-of-tolerance voltage conditions.

In order to make the flight telemetry subsystem response to telemetry mode change commands completely logical, the flight telemetry subsystem has removed all coupling between telemetry mode changes and engineering channel rate changes. The rate change command from the CC&S was therefore changed from a toggle with one command to a two-command *set–reset* pair of commands.

The attitude control pitch and yaw deadbands were reduced in half without any increased gas consumption, thus providing better antenna alignments and improved instrument-pointing accuracies.

Because of the deletion of the ultraviolet spectrometer covers, the pyrotechnic cover removal function was deleted also.

Due to a cold-welding problem in the infrared spectrometer motor gear train, the motor cannot be operated for 48 h in a vacuum environment. This posed a problem since all the science instruments are turned on at 48 h before encounter. To solve this problem, the signal from narrow-angle Mars gate 1, which occurs at approximately 35 min prior to encounter, is now used to start the motor, while at the same time initiating the cooldown. Ground command 49 backs up this narrow-angle Mars gate signal.

The centerline of the rocket engine was relocated to line up with the centerline of bay II as a direct result of the latest spacecraft center-of-mass determination.

Promethium 147 was eliminated from the spacecraft design as a source of heat because of its incompatibility with the ultraviolet spectrometer. Electrical heaters will be used to replace the promethium 147.

UNCLASSIFIED
CONFIDENTIAL

In order to reduce the forces imparted to the scan platform upon being unlatched, a pneumatic system was designed to latch it in four places at the same time. Release of the platform is effected when either CC&S command C5 or ground command 45 cause one valve squib to fire, releasing compressed gas. This will take place after the first maneuver.

The analog-to-digital wait state in the data storage subsystem was eliminated for sake of simplicity, and also because it is no longer required for a nominal mission.

The data storage subsystem no longer stops recording with the dropout of the data automation subsystem's sync signal. The data storage subsystem's recording turnoff is adequately backed up, and the sync-bar detecting circuitry was not considered reliable enough.

Ground command 16 was mechanized as a backup to the narrow angle Mars gate signal and the TV planet-in-view signal both to initiate the near encounter sequence in the data automation subsystem and to start recording in the data storage subsystem.

Scan platform telemetry assignments were changed to provide both clock and cone positions during cruise. Only cone position was directly available during cruise, prior to this change.

The ultraviolet spectrometer cover was eliminated at the request of the experimenter.

The analog tape recorder reference signal was deleted from the data automation subsystem because the TV signal now provides the needed reference.

The commands to be used to remove the solenoid-operated TV covers are CC&S command N7 backed up by ground command 46.

To prevent instrument damage from exposure to the sun, the TV shutters can be closed by ground command 48 prior to power turnoff.

A new scan-TV interface was established to reset the TV aperture control when cone slew occurs.

Hydrogen was chosen as the gas used for cooling the infrared spectrometer, and it was necessary to change the vessel material from titanium to aluminum.

Ground command 48, used to precondition the TV for power turnoff, is also used by the infrared radiometer to perform the same function.

a. Utilization of system capability. The following lists certain areas of spacecraft capability and the extent to which that capability is being utilized.

(1) Flight command subsystem

Direct commands: 49 out of a possible 53 are presently being used.

Quantitative commands: 4 out of a possible 4 are presently being used.

Coded commands: 1 out of a possible 1 is being used.

(2) Central computer and sequencer
Core: 128 of 128 words are being used.
Relays: 36 of 40 relays are presently being used.

(3) Engineering telemetry channels. 90 of 91 words are presently being used.

(4) Umbilical pins. 108 of 126 pins are presently being used.

(5) Packaging volume in octagon bays. 7800 $in.^3$ out of 8500 $in.^3$ are being utilized.

(6) Weight. 881 lb out of a 900-lb ceiling are presently in the design.

b. Spacecraft weight summary. Since the last quarterly design review, the spacecraft weight has increased by approximately 8 lb. The largest weight change was that associated with the removal of the promethium 147 heat sources and the subsequent addition of 20-mil cover glass to the solar panels. Other design changes (material change from titanium to aluminum for the infrared spectrometer gas bottles, reduction in the number of squibs and pinpullers required, addition of three accelerometer amplifiers and strengthening of the battery chassis) added another 3 lb. Finally, reductions totaling 5 lb (due to better design definition) brought the total net increase in the spacecraft weight to 8 lb. A summary of the weight changes by subsystem is presented in Table 3.

c. Spacecraft mass properties. The latest estimates of the mass properties of the spacecraft—that is, the center of mass, moments of inertia, and products of inertia—are contained in Table 4. A computer program has been developed to maintain these mass properties on a regular basis as the design firms up.

CONFIDENTIAL
UNCLASSIFIED

UNCLASSIFIED

Table 3. Launch weight summary

Subsystem	November 1966	March 1967	June 1967
Structure	180.1	170.4	195.9
Radio frequency	46.7	58.2	47.9
Flight command	10.0	11.4	7.5
Power	102.5	106.5	116.0
CC&S	18.0	24.0	24.0
Flight telemetry	21.9	22.4	24.0
Attitude control	57.3	59.6	59.6
Pyrotechnic	12.1	12.0	10.9
Cabling	55.8	68.7	71.2
Propulsion	45.2	46.4	46.5
Temperature control	22.4	38.3	30.8
Mechanical devices	42.4	43.1	44.2
Approach guidance	6.0	10.5	10.5
Data storage	38.0	38.0	34.2
Data automation	19.5	19.5	13.0
Scan control	12.6	18.3	18.3
Ultraviolet spectrometer	30.0	30.6	30.0
Television	45.6	47.6	46.8
Infrared spectrometer	24.4	29.0	31.0
Infrared radiometer	5.0	5.0	5.6
Total spacecraft design estimate	795.5	859.5	867.9
Engineering contingency	44.1	40.0	13.6
Total spacecraft weight	839.6	899.5	881.5

d. Spacecraft power status. Power requirements from several subsystems have increased appreciably since the last quarterly review. The major increases were:

(1) Radio frequency subsystem: 26.3 W in the high-power mode, and 22.3 W in the low-power mode.

(2) Temperature control: 5 or 15 W due to deletion of promethium, and depending upon whether the science platform temperature is at 0 or −10°C.

(3) Scan control subsystem: 18.5 W.

A tradeoff study was performed to try to reduce the power loads of the spacecraft, while at the same time increasing the capability of the solar panels to supply power under worst-case conditions.

The latter was accomplished by changing the 6-mil cover glass on the solar panels to 20-mil thickness, thereby gaining from 22 to 26 W in solar panel capability under maximum solar flare degradation. The loads have been

Table 4. Spacecraft mass properties

Property	At separation, prior to solar panel deployment	Cruise, before first maneuver	Unit
Centers of mass			
X_{cg}	−0.28	−0.28	in.
Y_{cg}	0.31	0.31	in.
Z_{cg}	−14.51	−8.98	in.
Moments of inertia			
I_x	131.42	111.89	slug-ft^2
I_y	157.35	141.47	slug-ft^2
I_z	73.98	185.93	slug-ft^2
Products of inertia			
I_{xy}	−1.69	−1.69	slug-ft^2
I_{xz}	0.043	0.31	slug-ft^2
I_{yz}	3.54	3.24	slug-ft^2

reduced by several methods—first, by connecting heaters to the reset side of the data storage subsystem power relay, saving approximately 25 W of power during playback; second, by incorporating a direct command to toggle the thermostatic heaters between the battery and the dc bus; and third, by reduction of the platform temperature from 0 to −10°C which saves 10 W of heater power.

2. Alternative Actions for Improving Solar Panel Power Margins

As a result of recent additions to the spacecraft power demand, the spacecraft solar panel power margin has a possibility of becoming negative during all the optional or "nonnominal" encounter and playback modes. This would mean entering the battery-sharing mode. This article will describe possible alternatives for improving the power margins during those phases of the mission, so that battery sharing becomes less likely to occur.[1]

With the present spacecraft configuration, the power margins for six different modes of encounter and playback are as presented in Table 5. These margins reflect (1) the additional 10 and 13 W required for the TWTAs in the low and high power modes, respectively, and (2) the 15 W of dc heater power required to replace the promethium radio-isotope heat sources. (Fifteen watts are all that are needed even in the worst-case condition—worst case pertaining to the effective emittance of the

[1]Since the emphasis in this article centers around the possibility of entering the battery-share mode, it is also appropriate to consider how long the battery could sustain share-mode operation during encounter. Section 3 is an analysis of this, assuming that the spacecraft had entered the battery-share mode and was in a gyros-on, low-power TWT mode.

UNCLASSIFIED

UNCLASSIFIED

Table 5. Solar panel power margins in present configuration

Mode	Gyros	Traveling wave tube	Power demand, W	Solar panel power margins, W					
				No flare			Maximum flare		
				Highest solar panel performance	Nominal solar panel performance	Lowest solar panel performance	Highest solar panel performance	Nominal solar panel performance	Lowest solar panel performance
1. Encounter	Off	Low	358	205	164	122	64	33	2
2. Playback[a]	Off	High	353	210	169	127	69	38	7
3. Encounter	On	Low	395	168	127	85	27	− 4	−35
4. Encounter	On	High	426	137	96	54	− 4	−35	−66
5. Encounter	Off	High	389	174	133	91	33	2	−29
6. Playback[a]	On	High	389	174	133	91	33	2	−29
[a]Actually, the playback margins would be worse than those shown if playback were to continue through encounter + 16 days. If this occurs, (and it *is* a distinct possibility) then instead of 69 mW/cm² being incident on the solar panels, only 65 mW/cm² would be incident (due to the increased distance from the sun). This would mean a 6% drop in the available solar panel power, and the margins for the two playback modes mentioned above drop to the following:									
2. Playback	Off	High	353	177	139	99	44	15	−14
6. Playback	On	High	389	141	103	63	8	−21	−50

platform thermal shielding.) The minus numbers in Table 5 indicate that the power demand for that mode exceeds the solar panel supply (given that particular set of assumptions) by the amount indicated. As can be seen, all the optional or nonnominal modes shown have a possibility of entering the battery-sharing mode.

a. Substitution of 20-mil cover glass. With the solar panels in their present configuration (6-mil cover glass), the solar panel power output before any solar flare degradation is equal to 522 W with a manufacturing tolerance of ±8%. Thus, it varies from

480 to 522 to 563 W
(low) (nominal) (high)

After *maximum* solar flare degradation (25% for 6-mil cover glass), these figures reduce to

360 to 391 to 422 W
(low) (nominal) (high)

With 20-mil cover glass on the solar panels, the solar panel power output before any solar flare degradation is equal to the power in the 6-mil case, less 3.5% (due to the added thickness of the glass) or

463 to 504 to 543 W
(low) (nominal) (high)

After *maximum* solar flare degradation (17.5% for 20-mil cover glass) these figures reduce to

382 to 416 to 448 W
(low) (nominal) (high)

Thus it can be seen that the addition of the 20-mil cover glass would mean a gain of from 22 to 26 W (assuming maximum solar flare degradation) for all phases of the mission.

The impact of the added weight on the spacecraft would be as follows:

Increase due to thicker glass:	12 lb
Increase due to structural changes:	2 to 4 lb
Decrease due to Pm 147 removed:	−9 lb
Increase due to electrical heaters circuitry:	1 lb
Total increase in weight	6 to 8 lb

b. Reduction of science platform temperature from 0 to −10°C. The decision to operate the instruments under the thermal blanket at 0°C was the result of a compromise between two of the three instruments under the blanket—the TV and the infrared radiometer (IRR). (The ultraviolet spectrometer (UVS) was more flexible thermally.) It is desirable to operate the TV as near to room temperature as possible, primarily to test and calibrate without needing to enter a cold chamber to do so. The IRR operated from approximately −20 to 0°C. Thus, 0°C was an agreeable compromise at the time the decision was made.

The platform is presently heated to 0°C by thermostatically controlled, dc-powered heaters that require 0 to 23 W, and 15 W maximum of constant heat formerly supplied by Pm 147 (electrical heaters are planned as the Pm 147 replacement). If the equilibrium temperature of

UNCLASSIFIED

UNCLASSIFIED

the platform was lowered to −10°C, an estimate by the temperature-control engineer indicated that the 15-W figure could be reduced to 5. Therefore, the net power saving by lowering the temperature would be 10 W.

A quick check indicated that the major consequence of a lower temperature would be that additional funding would be required because the testing and calibrating of the TV and possibly the UVS would have to be accomplished in a cold chamber facility. At present, there does not seem to be any significant mechanical or electrical problems with this. However, the experimenters are presently being consulted for confirmation.

c. Additional direct command capability to switch heaters. Consideration was given to providing a direct command capability for switching a block of heaters from the dc bus directly onto the battery, in an attempt to share the load if it proves excessive during encounter. The two heater loads which are on during encounter were investigated and the effect on the platform temperature of switching them onto the battery is summarized in Table 6.

It may be concluded from Table 6 that a total of 23 W could be gained (by switching the dc thermostatic heaters onto the battery) without serious degradation to the performance of the instruments *even if* the nominal platform temperature were reduced to −10°C. In the worst case, the platform temperature would drop to −23°C. The TV is the only instrument in trouble at this temperature. The TV is presently mechanized to operate acceptably with a lower encounter temperature limit of −20°C, *but* if the nominal platform temperature were to be reduced to −10°C, this lower temperature limit would probably be lowered somewhat.

The command has the additional benefit of providing a means whereby the condition of the battery could be checked out in flight.

The direct command capability could be made available from the flight control subsystem. It would toggle a relay to switch the dc thermostatic heaters back and forth between the dc bus and the battery. The switching would be accomplished by the power subsystem. However, since there is no available space in the present power distribution module in case 1, another module would have to be added. There is room in the case for this additional module. (This module would be the same one presently being planned on for heater fuses. It is logical therefore that the entire module become the responsibility of the power subsystem engineers and they have agreed to this should a decision be made to add the switching capability.)

d. Addition of a second battery to increase confidence in battery sharing. A redundant battery had been considered for some time by the power subsystem engineers should battery sharing become likely during the later portions of the mission.

The battery proposed uses the same cell type and quantity of cells as the main battery, and would require additional switching and control circuitry packaging with it. Therefore, it would weigh somewhat more than the present battery (which weighs approximately 37 lb) and would take more volume, although the configuration could be different to accommodate mounting.

Table 6. Platform temperature effects of switching heaters onto battery during encounter

Heaters being switched	Constant dc heaters (the Pm 147 replacement)			Thermostatic dc heaters			
Nominal platform temperature	0°C	0°C	−10°C	0°C	0°C	−10°C	−10°C
Amount of heat generated before switching, W	15	15	5	23	23	23	23
Amount of heat generated after switching, W	6	6	2	9	9	9	9
Effective emittance of blanket[a]	Nominal	Worst	Mechanization not worthwhile for only 5 W	Nominal	Worst	Nominal	Worst
Resultant new temperature	0°C[b]	−6°C		0°C[b]	−11°C	−10°C[b]	−23°C

[a]Nominal effective emittance: 0.10; worst case = 0.12.

[b]Temperature remains the same because it is within the regulating range of the thermostatic heaters.

UNCLASSIFIED

UNCLASSIFIED
CONFIDENTIAL

There is no requirement to recharge this battery. It would be switched on-line only on command prior to a peak load condition, or when called upon to do so by its own monitoring circuitry. However, nonrechargeable high-energy-density primary cells were not investigated for this application because they were not qualified.

In view of the weight and interface complexity of the proposed additional battery, it is not at all clear that it is one of the desirable or even feasible solutions to the problem at hand, but it may be necessary, however costly, if other solutions are inadequate.

e. Connection of cruise heaters to backside of DSS relay. The present plans for heater circuitry for the spacecraft are shown in Fig. 1. As can be seen, heaters in the instruments dissipating 39.7 W are connected to the backside of the encounter relay. This means that these heaters are on during cruise, off during encounter, and on again during playback. Since the playback power margin could stand improvement, these heaters could be connected to the backside of the data storage subsystem (DSS) relay instead, and thus be off during playback. This would save approximately 50 W (39.7 plus efficiency drops in the booster regulator and inverter) during the playback portion of the mission.

Such a connection is available in the power subsystem. It would not impact upon the spacecraft weight.

The reason for not connecting all the 2400 Hz on the backside of the DSS relay is that the minimum load requirement on the 2400-Hz inverter (125 W) could not be met during playback if this were done.

The reason for suggesting that the instrument heaters, rather than the heaters in the bays, be placed on the backside of the DSS relay is that from a temperature-control point of view, it would be better to have heat in the bays during playback, rather than heat in the platform.

The disadvantage of this proposal is that if it is desired to execute a mock encounter and playback sequence somewhere between the maneuver and the real encounter, then the time the spacecraft could be in the playback mode would definitely be limited. Otherwise, the platform temperature would drop below the minimum storage temperature of the instruments. According to the temperature-control engineer, this does not present a problem during the thermal testing on lab, because supplementary heaters could easily be set up.

This problem could be circumvented by switching only 20 "heater watts" to the backside of the DSS relay instead of all 39.7 W. This would still mean a gain of 25 W during playback. The number of watts left on would be enough to keep the platform above the minimum storage temperature of $-30°C$ even if the nominal platform temperature were to be reduced to $-10°C$ and if we assume worst-case platform shielding.

f. Locating a suitable radioactive replacement for Promethium 147. Presently JPL Section 294 is searching for a satisfactory radioactive heat source to replace Pm 147. Preliminary information, however, indicates that there is not any obvious replacement.

Thus, it can be said that it would be highly questionable whether a full far-encounter period would be performed if battery sharing were indicated; but in all likelihood a near-encounter period would be attempted even if sharing were indicated.

Another consideration worth mentioning is that even if the full 900 W-h were taken from the battery (presumably indicating that the battery was healthy and performing) there is no guarantee whatsoever that it will then properly accept and retain a charge from the battery charger. This means that if the full capacity were used up at encounter, it might not be possible to replace it to provide reserve power capability during playback.

g. Summary and recommendations. After studying Table 7, it was recommended that Nos. 1, 2, 3, and 5 (b) be incorporated. Number 1 speaks for itself—of all the alternatives, it gains the largest amount of power and appears feasible from all technical points of view. Numbers 2 and 3 are also feasible and gain 10 and 23 W, respectively. Number 3 also gains the battery check-out capability, which is extremely desirable. Number 4 is eliminated from practical consideration due to its weight and interface complexity. Number 5 (b) is recommended because it is felt that the constraint mentioned in the discussion is worthwhile to consider and 25 W is still a significant gain during playback. Number 6 is not an alternative.

Incorporation of the recommended alternatives would yield the power margins given in Table 8. In addition to the margins shown, they would increase by 23 W whenever the toggle for the heaters was in the battery position.

The *Mariner* Mars 1969 Project Office provided immediate authorization to proceed with recommendations

UNCLASSIFIED
CONFIDENTIAL

UNCLASSIFIED
CONFIDENTIAL

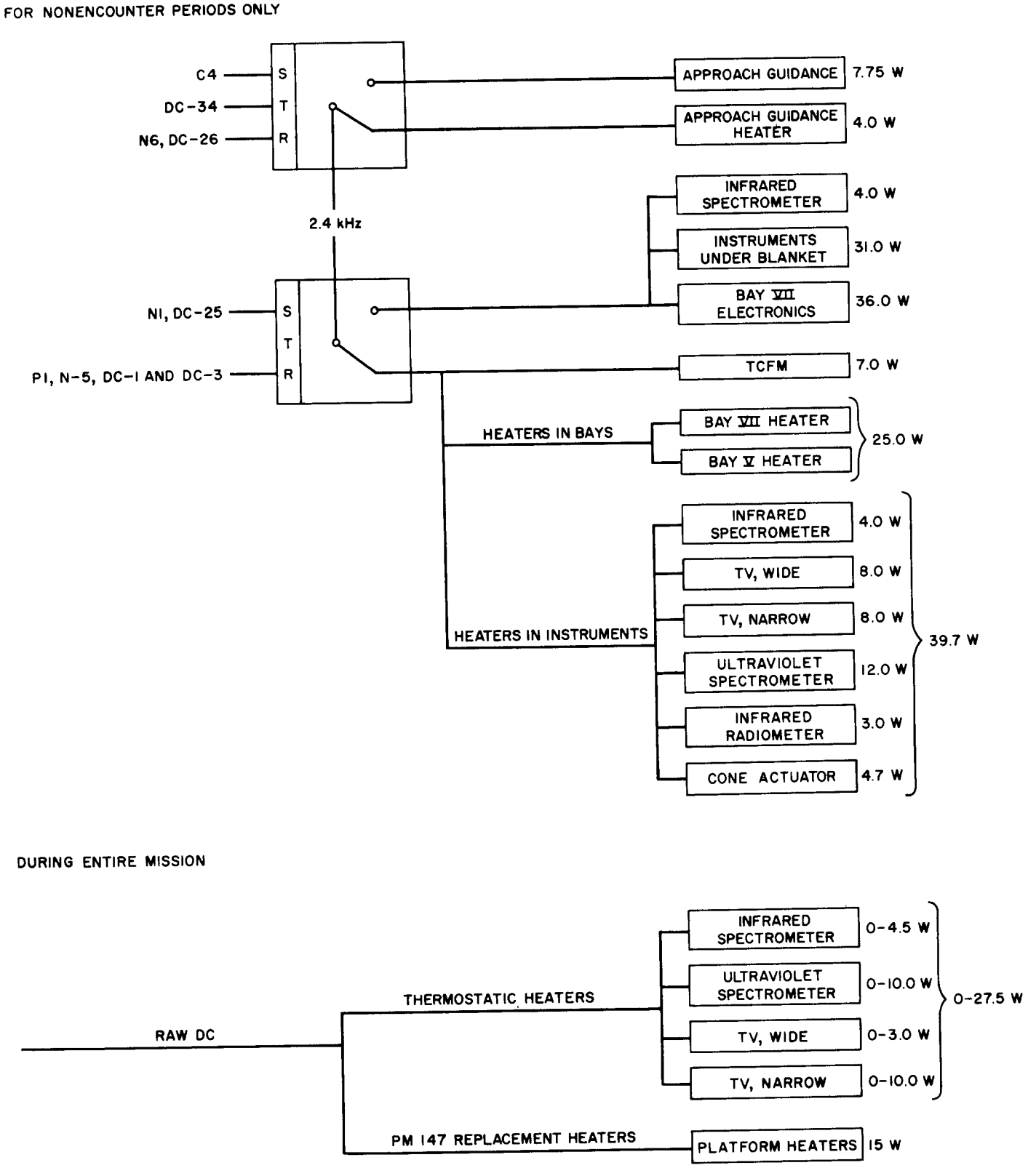

Fig. 1. Spacecraft heater circuitry (present configuration)

UNCLASSIFIED
CONFIDENTIAL

UNCLASSIFIED

Table 7. Alternatives and gains

Alternatives	Gains
1. 20-mil cover glass	From 22 to 26 W during all phases
2. Reduction of platform temperature	10 W during all phases
3. DC to toggle thermostatic heaters between the battery and the dc bus	0–23 W whenever the toggle is in the battery position plus a means to make in-flight checks on condition of battery
4. Additional battery to increase confidence	Increased confidence in battery sharing
5. Connection of heaters to backside of DSS relay	(a) 50 W during playback if *all* the instrument heaters are placed on the DSS relay (b) 25 W during playback if *half* the instrument heaters are placed on the DSS relay
6. Replacement of Pm 147 with another radioactive heat source	Not applicable, since no source can be located

providing for (1) substitution of 20-mil cover glass, (2) an additional direct command capability to switch heaters onto the battery, and (3) the connection of the cruise heaters to the backside of the data storage subsystem power relay. Another recommendation, involving the reduction of the scan platform temperature from 0 to −10°C, was studied further, determined feasible, and is also being implemented in the design.

3. Share Mode at Encounter

The emphasis on avoiding share-mode operation was the central theme of the foregoing article; now it is appropriate to consider how long the battery could sustain share-mode operation during encounter. (The particular case looked at assumed gyros-on and low-power TWT, and 6-mil cover glass.)

The solar cell configuration now planned is a 78- × 224-cell array for each panel. This provides roughly the following power at Mars encounter (low-limit, or "guaranteed" power) at 25 V, the battery-share voltage:

Panel degradation	Volts	Amperes	Power, W
0	25	14.1	352
22%[2]	25	10.7	267

The spacecraft average or quiescent power load during far encounter, for gyros on, but low-power TWT operation (with the platform temperature reduced to −10°C nominal) equals 361 W; this means the battery must furnish what the solar panel cannot—in this case 9 W if the panels are undegraded and 94 W if they are 22% degraded.

Clearly, then the battery would have to supply 48 h × 9 W = 432 W-h with no solar panel degradation at all, and more than ten times that figure if they are fully degraded. The guaranteed battery capacity at encounter is 900 W-h.

For near encounter under the same conditions (gyros on, low-power TWT) 370 steady-state W are required.

[2]Curves for 25% degradation (project worst-case model) were not available. The "percent degradation" refers to the panel's maximum power point and so may not correspond to the 25-V point.

Table 8. Power margins with incorporation of recommended alternatives

Mode	Gyros	Traveling wave tube	Power demand, W	Solar panel power margins, W					
				No flare			Maximum flare		
				Highest solar panel performance	Nominal solar panel performance	Lowest solar panel performance	Highest solar panel performance	Nominal solar panel performance	Lowest solar panel performance
1. Encounter	Off	Low	348	195	156	115	100	68	34
2. Playback[a]	Off	High	318	225	186	145	130	98	64
3. Encounter	On	Low	385	158	119	78	63	31	− 3
4. Encounter	On	High	416	127	88	47	32	0	−34
5. Encounter	Off	High	379	164	125	84	69	37	3
6. Playback[a]	On	High	354	189	150	109	94	62	28
[a]If playback lasts up to encounter + 16 days, the following playback margins are applicable:									
2. Playback	Off	High	318	193	157	117	104	74	41
6. Playback	On	High	354	157	121	81	68	38	5
Each margin shown would be improved 23 W whenever the toggle for the dc thermostatic heaters is in the battery position.									

UNCLASSIFIED

The battery would then have to furnish 370 − 352, or 18 W assuming no degradation, or 370 − 267, or 103 W assuming 22% degradation. If these near-encounter loads exist for, say, 3 h (1 h prior to closest approach and 2 h after) then 36 W-h would be required from the battery with no degradation, or 309 W-h with 25% degradation.

4. Launch Vehicle Integration

In a continuing program to achieve and document interface design agreements, this reporting period has included the release of spacecraft/launch vehicle interface schedules; the establishment of a mutually agreeable test documentation development plan; the release of seven amendments to the interface control document; the distribution of a very preliminary version of the electrical interface control drawing; and the release of two changes against the mechanical interface control drawing.

The interface schedule document contains the schedules necessary to accomplish the integration of the spacecraft system with the launch vehicle system. The schedules are negotiated through the hardware interface panel, agreed to by JPL and LeRC, and structured to conform with official NASA Flight Schedules and *Mariner* Mars 1969 Project milestones.

The test documentation development plan calls for the development and implementation of interface test plans, procedures, and reports for: match mate; pyrotechnic compatibility tests; and combined systems test.

C. Guidance and Control

1. Introduction

Release of prototype design drawings for the *Mariner* Mars 1969 attitude control and scan control subsystems has progressed and all drawings are now released except for one of the scan electronics subassembly package and one printed wiring board assembly for the Canopus sensor. Design Requirement Documents have been released for the scan control, and approach guidance subsystems.

Utilization of the increased capability of the *Mariner* Mars 1969 Canopus sensor has resulted in some simplification of the attitude control electronics. In particular, the bias signal used to position the sensitive region in the Canopus sensor to one side of the field of view during roll search has been applied to the electronics as the roll search signal itself. This has allowed the removal of the roll search generator elements from the electronics unit and has simplified the interface between the Canopus sensor and the electronics.

The dead band size for the attitude control switching amplifiers has been reduced for the pitch and yaw axis from ±8.5 to ±4.0 mrad. This change provides for more accurate attitude orientation of the spacecraft during cruise and trajectory correction maneuvers. The more accurate attitude control will benefit high-gain antenna pointing, scientific instrument pointing, and will improve the expected accuracy of trajectory correction maneuver. Analysis has shown that this change should not increase attitude control nitrogen gas consumption unless residual torques on the spacecraft are less than 10 dyn cm.

Fabrication of attitude control and scan control production prototype hardware has started at Minneapolis Honeywell. Fabrication of engineering prototype models has been initiated on all scan subsystem hardware and the Canopus sensor. Developmental vibration testing has started on the Canopus sensor engineering prototype housing.

2. Attitude Control Subsystem

The Kearfott C702565001 miniature floated rate integrating gyroscope has been selected for use in the attitude control subsystem. Procurement of the gyros, which was initiated in mid-1966, incorporates many new technical requirements representing significant improvements over JPL gyro procurements for previous programs. Generally these new requirements represent an increased effort by JPL to ensure the quality and uniformity of gyros intended for flight hardware use.

The required quantity of 24 gyros is being provided in a single lot and will be furnished to the subsystem contractor as government-furnished equipment. Project engineers and quality assurance engineers have been assigned both at Kearfott and JPL.

A design review of the gyroscope which Kearfott supplied to JPL for the *Mariner* Mars 1964 program was conducted, including a review of the mechanics, electronics, environments and controlling process, procedure and operation sheets. Recent development and qualification of new gyros for other applications supplied improvements in mechanical design which resulted in improved drift performance, simplification of fabrication and increased reliability. The most significant of these changes are flex-lead attachment, mass adjustment simplification, and removal of possible contamination sources. Kearfott requested the incorporation of these changes into *Mariner* Mars 1969 gyros; this has been approved.

UNCLASSIFIED
CONFIDENTIAL

Formalized NASA quality requirements (applicable portions of the requirements of NASA Quality Publication NPC 200-2) have been imposed on this procurement. The requirements include a formal Quality Program Plan, monthly Quality Status Reports, formal failure reporting on all gyros failing final test, and approval control on all changes in gyro design, material, manufacturing processes, manufacturing procedures and testing.

Particle contamination of gyro gimbal floatation fluid and the area in which this fluid circulates is a critical problem in floated gyroscopes and if not controlled can result in problems ranging from variable gyro drift performance to total failure. To control this contamination to an acceptable level and type for the *Mariner* Mars 1969 program, Kearfott has redesigned filling fixtures, updated operation sheets, and removed contamination sources from within the gyro. JPL has established a gyro group-sampling program wherein the manufacturer accepts rework responsibility for contaminated units. This program consists of separating final gyro assembly and test into groups of six units, and evaluating the contamination level and type in one gyro from each group. The specified maximum permissible particle count imposed on the group sample gyro is 0.001 to 0.002 in., 150 particles; 0.002 to 0.004 in., 28 particles; 0.004 to 0.008 in., 10 particles; total count, 188 particles.

Should the sample unit fail the particle level requirements, it is specified that all assembled gyros of that group will be disassembled down to the gimbal assembly, recleaned, and subsequently rebuilt. A two-part particle contamination specification imposes the tightest control on the group sample gyro before it leaves the clean room, and then imposes a relaxed particle count for 2 yr or 2000 h of operating warranty life. If, during this warranty period, the gyro fails for reasons relating to particle contamination and subsequently at disassembly fails the contamination specification, the manufacturer has accepted responsibility for rework. Evaluation of general workmanship is also required on one unit from the entire lot; this is accomplished by disassembly evaluation of a completed gyro down to the fluid seal. Evaluation of the gimbal assembly is accomplished by disassembly of a completed gimbal down to the motor. Corrective action indicated by these lot samples will subsequently be taken as required.

The inherent design of gyro spin motors using ball bearings causes them to become a critical part in the reliability of the gyroscope. The most common failure mode is for the motor to fail to synchronize at its designed operating speed of 24,000 rev/min. To assure special care in this area, JPL has required Kearfott to initiate a spin motor selection program, the basic concept of which is to start 40 motor assemblies into fabrication test to produce 27 selected motors. Three sequential selections of the best units are then made using the time between to apply three special evaluation tests. These include run up and run down time at 115°F; run up at 50°F; and spin motor power evaluation. The latter consists of recording one phase of spin motor current for a specific period of time and evaluating the number and amplitude of recorded discontinuities. The final motor-gimbal assemblies are chosen by board members, comprised of vendor representatives from reliability, quality assurance, production and engineering, and JPL.

Gyro gimbal stiction is another phenomenon known to be critical to reliable gyro performance. Gimbal stiction is defined as an intermittent increase in gimbal friction, thought to be related to floatation fluid particle contamination, and has been found to be an elusive and difficult condition to uncover by specific gyro testing. A new acceptance test, entitled gimbal freedom test, was prepared by JPL and has been imposed as a requirement of acceptance testing at Kearfott. This test is performed with a low-gain electronic loop used to maintain the gyro gimbal at electrical zero. The output voltage from the gyro pickoff and a ramp generator are summed at the input of the electronic loop ac amplifier. In the event that the ramp generator output exceeds the gyro pickoff signal, an output from the electronic loop dc amplifier will result, indicating a change in gimbal friction. The gyro specification provides for a limit on the time during which this friction may exist, and also on the amplitude that the friction level may attain.

Experience gained from previous flight programs relating to the importance of data correlation indicates that similarity of test equipment is very important. Therefore, JPL is supplying the manufacturer with gyro loop-closure electronics, built from circuits identical with the flight hardware, to be used for all acceptance testing. This approach to testing is expected to also reduce the problems of data correlation between testing at the single gyro and subsystem levels. Acceptance tests performed on gyros at JPL for the *Mariner* Mars 1964 program used digital readout equipment to record gyro rebalance current as a function of gyro drift rates. This was accomplished by inserting a precision resistor in series with the torquer rebalance circuit, and subsequently converting the voltage drop across the resistor to pulses, using a voltage-to-frequency converter. The past method of data

UNCLASSIFIED
CONFIDENTIAL

recording at Kearfott consisted of an analog strip chart recording, and visual interpretation of the data. The digital method which has now been imposed on Kearfott will increase the capability to resolve the data by two orders of magnitude.

The normal quantity of acceptance testing performed at Kearfott has been increased by the same amount which in the past was accomplished at JPL. By placing a JPL quality-assurance representative with extensive inertial component training in residence to witness testing, total confidence in the acceptability of the gyro has been obtained. This additional gyro evaluation is called Flight Evaluation Testing and consists of two major functions. The first is the eight-position heading test which is performed eight times a day for 5 days. The second is the equatorial tumble test which is performed four times a day for 2 days. At the conclusion of this phase of gyro evaluation the gyro is hand-carried to JPL.

To increase confidence even further in the flight readiness of this gyro, JPL is conducting a prequalification test program. This program, which includes receiving inspection, type-approval environment and post environmental testing, is now being imposed using the first *Mariner* Mars 1969 gyro delivered to JPL. The type-approval test content and level is essentially that specified in the JPL *Mariner* Mars 1969 environmental test specification.

Fabrication at Kearfott is complete on 34 motor assemblies, 27 motor-float assemblies and 13 gyroscopes. To date, only two gyros have been rejected from final test for failure to meet performance requirements. These gyros are presently undergoing extensive investigation to determine cause of failure and required corrective action. Presently one gyro is in the initial calibration phase at Kearfott and one is in final test in preparation for delivery to JPL. Major milestones have been passed by the first, second, and third groups of gyros in that all three group sample gyros were well within the particle contamination requirements.

The gyro detail specification ES 500603A has recently been revised at JPL to include the updated *Mariner* Mars 1969 environmental specification, as well as revisions to the gimbal freedom and equatorial tumble test requirements. The four required sets of test equipment, including all necessary drawings and equipment calibration procedures, have been delivered to the gyro manufacturer. Kearfott has placed this equipment into four test stations which have been subsequently qualified by functionally testing a representative gyro. The present plan to subject the first gyro to a full evaluation program at JPL, including the *Mariner* Mars 1969 type-approval test, is moving along in a satisfactory manner. Data taken to date confirm that the gyroscope is operating within the specification limits.

This procurement is progressing nominally according to schedule, with the first five gyros now in test at JPL.

3. Scan Control Subsystem

a. Introduction. Figure 2 is a block diagram of the scan control subsystem. The dotted lines show the six basic blocks that constitute the subsystem: the stepper motor drive electronics, slew logic, servo amplifier, far encounter planet sensor, power supply and actuators. A general discussion of the scan platform subsystem is contained in SPS 37-44, Vol. II (Confidential). The following articles are a more detailed description of the stepper motor drive electronics and the servo amplifiers.

b. Stepper motor drive electronics. The *Mariner* Mars 1969 scan control subsystem has the capability of storing platform pointing information in the form of discrete clock and cone angles. At encounter this stored information is used to drive the platform to a corresponding position.

The mechanization selected to implement this requirement utilizes a stepper motor-driven potentiometer as the memory device. The stepper motor has the characteristic that it rotates 90 deg in either a clockwise or counterclockwise direction, depending upon the position of the motor rotor with respect to the stator at the time of the signal input, and the motor winding energized. The requirement for the subsystem to maintain the stored positional information in the presence of power transients would ordinarily dictate the need for a nonvolatile memory to store the motor position at any point in time. The scan electronics have been mechanized to cause the motor to increment a full ± 360 deg per step input, thus alleviating the motor position as a variable and eliminating the need for a memory unit. This is accomplished by generating an ordered sequence of 4 pulses per each 1-pulse input to the subsystem. The order in which the sequence occurs will cause the motor to increment in either clockwise or counterclockwise direction.

Logic conventions. All logic diagrams in this article (except Fig. 3) are drawn so they represent the hardware used to fabricate the circuits (Signetics series SE). The

SSIFIED

the first gyro to a full evaluation program at JPL, including the *Mariner* Mars 1969 type-approval test, is moving along in a satisfactory manner. Data taken to date confirm that the gyroscope is operating within the specification limits.

This procurement is progressing nominally according to schedule, with the first five gyros now in test at JPL.

3. Scan Control Subsystem

a. Introduction. Figure 2 is a block diagram of the scan control subsystem. The dotted lines show the six basic blocks that constitute the subsystem: the stepper motor drive electronics, slew logic, servo amplifier, far encounter planet sensor, power supply and actuators. A general discussion of the scan platform subsystem is contained in SPS 37-44, Vol. II (Confidential). The following articles are a more detailed description of the stepper motor drive electronics and the servo amplifiers.

b. Stepper motor drive electronics. The *Mariner* Mars 1969 scan control subsystem has the capability of storing platform pointing information in the form of discrete clock and cone angles. At encounter this stored information is used to drive the platform to a corresponding position.

The mechanization selected to implement this requirement utilizes a stepper motor-driven potentiometer as the memory device. The stepper motor has the characteristic that it rotates 90 deg in either a clockwise or counterclockwise direction, depending upon the position of the motor rotor with respect to the stator at the time of the signal input, and the motor winding energized. The requirement for the subsystem to maintain the stored positional information in the presence of power transients would ordinarily dictate the need for a nonvolatile memory to store the motor position at any point in time. The scan electronics have been mechanized to cause the motor to increment a full ±360 deg per step input, thus alleviating the motor position as a variable and eliminating the need for a memory unit. This is accomplished by generating an ordered sequence of 4 pulses per each 1-pulse input to the subsystem. The order in which the sequence occurs will cause the motor to increment in either clockwise or counterclockwise direction.

Logic conventions. All logic diagrams in this article (except Fig. 3) are drawn so they represent the hardware used to fabricate the circuits (Signetics series SE). The

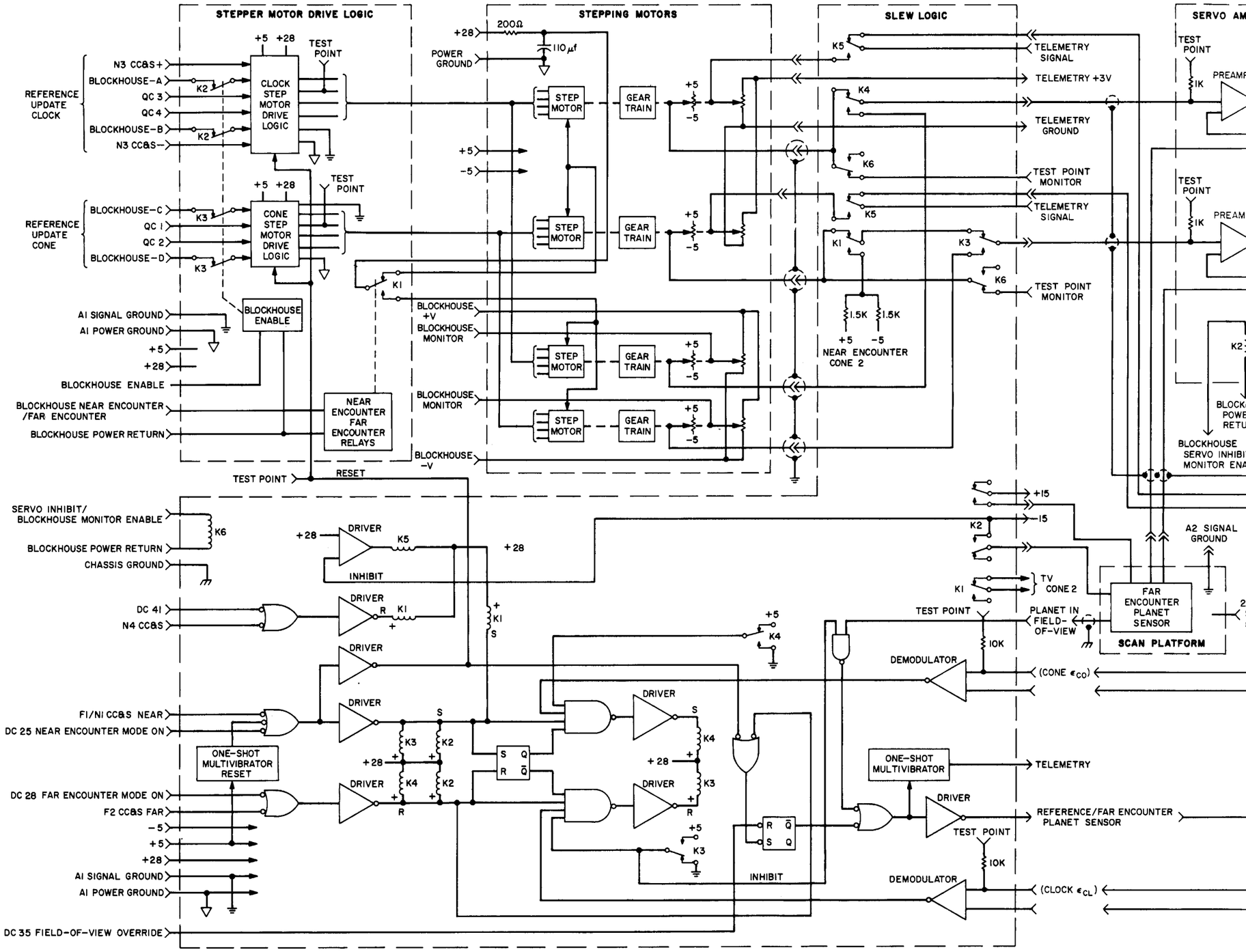

JPL SPACE PROGRAMS SUMMARY 37-46, VOL. II

SSIFIED

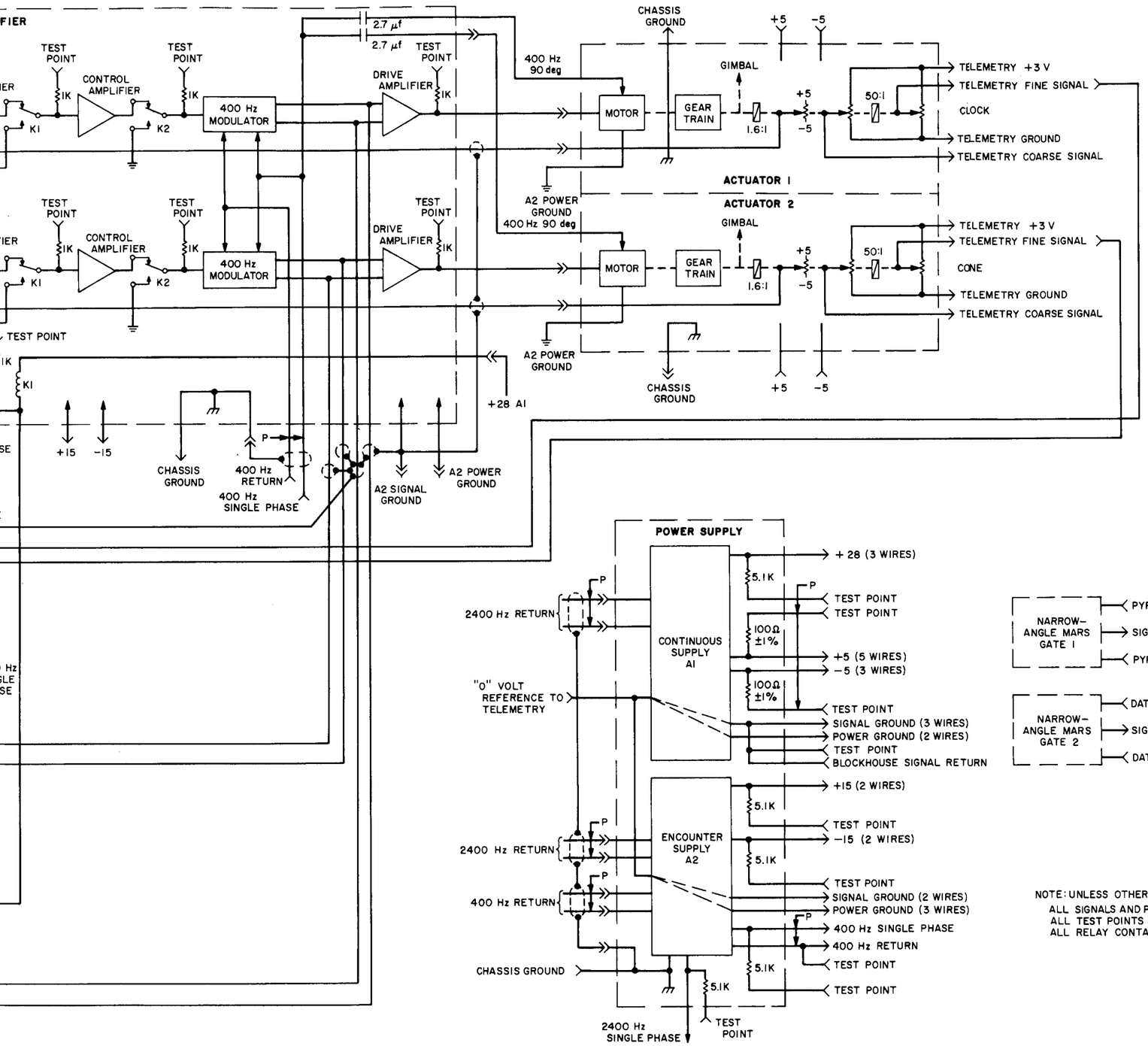

Fig. 2. Scan control subsystem

ASSIFIED

UNCL

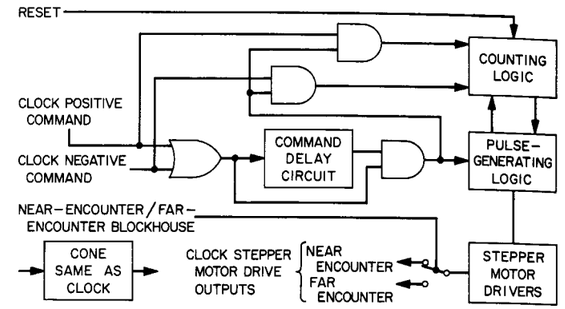

Fig. 3. Stepper motor drive electronics functional block diagram

"1" logic level is represented by either a high voltage (+5) or an open circuit in these logic elements. The "0" logic level is represented by a ground. These are the signal definitions which are used in the circuit description.

The basic logic element of the Signetics SE line is the *nand* gate. The flip-flop conventions are represented in Fig. 4 (b) and (c). Figure 4 (b) shows the representation of the SE 124 G reset-set (R-S) flip-flop. Note that the clock input of this flip-flop is ac-triggered. Figure 4 (c) illustrates how a dc R-S flip-flop may be fabricated using two *nand* gates.

The one-shot convention is illustrated in Fig. 4 (d). The one-shot multivibrator is also ac-triggered.

Functional description. Figure 3 is a functional block diagram of the stepper motor drive electronics. Shown in some detail is the clock channel. The cone channel, represented by a simple block, is identical to the clock channel.

An input signal is channeled along parallel paths to pulse generating logic and counting logic. The command delay circuit serves to discriminate against noise and relay chatter, as discussed in a subsequent paragraph. The counting logic, upon initiation through an input pulse, counts to four in one of two ways, depending upon whether a positive or negative command is imposed on the circuit. The pulse generating logic, acting upon input signals and the counting logic signals, generates four pulses for each one input pulse. The stepper motor drivers raise the generated pulses to the proper power level to allow the stepper motor to be driven. The relay shown on the output allows both the near encounter and the far encounter clock angle to be driven from the same elec-

UNCL

UNCLASSIFIED

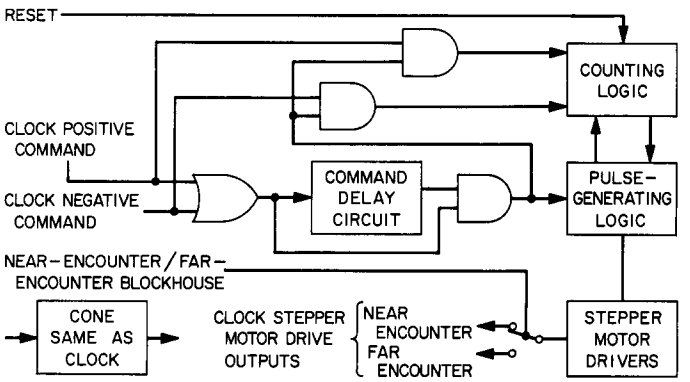

Fig. 3. Stepper motor drive electronics functional block diagram

"1" logic level is represented by either a high voltage (+5) or an open circuit in these logic elements. The "0" logic level is represented by a ground. These are the signal definitions which are used in the circuit description.

The basic logic element of the Signetics SE line is the *nand* gate. The flip-flop conventions are represented in Fig. 4 (b) and (c). Figure 4 (b) shows the representation of the SE 124 G reset-set (R-S) flip-flop. Note that the clock input of this flip-flop is ac-triggered. Figure 4 (c) illustrates how a dc R-S flip-flop may be fabricated using two *nand* gates.

The one-shot convention is illustrated in Fig. 4 (d). The one-shot multivibrator is also ac-triggered.

Functional description. Figure 3 is a functional block diagram of the stepper motor drive electronics. Shown in some detail is the clock channel. The cone channel, represented by a simple block, is identical to the clock channel.

An input signal is channeled along parallel paths to pulse generating logic and counting logic. The command delay circuit serves to discriminate against noise and relay chatter, as discussed in a subsequent paragraph. The counting logic, upon initiation through an input pulse, counts to four in one of two ways, depending upon whether a positive or negative command is imposed on the circuit. The pulse generating logic, acting upon input signals and the counting logic signals, generates four pulses for each one input pulse. The stepper motor drivers raise the generated pulses to the proper power level to allow the stepper motor to be driven. The relay shown on the output allows both the near encounter and the far encounter clock angle to be driven from the same electronics. Figure 5 is a detailed logic diagram of the stepper motor drive electronics.

Command delay circuit. The mechanics of the noise discrimination circuit are best illustrated by referring to Fig. 6, which is a timing diagram illustrating the labelled points in Fig. 5. The response of the circuit to two types of inputs is illustrated. First, a narrow pulse input representative of a noise spike is introduced into the circuit; as is shown, *E*, the output of the noise discrimination circuit, does not change state. *H* takes the pressure of an input signal 15 ms (time constant of one-shot multivibrator 1) after the signal first appears for flip-flop 1 (FF 1) to turn over. Valid input commands have a minimum pulse width of 75 ms.

Pulse generating logic. The pulse generating logic uses two monostable multivibrators (OS 2 and 3) and associated control logic. A timing diagram for the pulse generating logic is presented in Fig. 7. OS 2 is triggered the first time when FF 1 is reset (trailing edge of input command). OS 2 is set at a nominal pulse width of 70 ms. The output of OS 2 is used to increment the counting logic by one count and to trigger OS 3 (both of these actions occur on the trailing edge of the OS 2 output). OS 3 is set at a nominal pulse width of 35 ms. The first three output pulses for OS 3 are returned to the input of OS 2 through counter-controlled gates. The fourth output pulse of OS 3 is transmitted only to the appropriate stepper motor drive circuit.

The pulse generating logic therefore generates a sequence of four output pulses to the stepper motor drive electronics. The sequence of the pulses is controlled (see following paragraph) so that the stepper motor rotates through 360 deg in either a clockwise or counterclockwise direction.

Counting logic. The counting logic consists of a control flip-flop (two *nand* gates), two ac-triggered flip-flops (FF 2 and 3), and associated gating. Figure 7 contains a timing diagram for this logic. The control flip-flop is set 15 ms after an input command is received by the *and* of the input command and a signal from FF 1. This control flip-flop controls the sequence in which the counting circuit counts. The two flip-flops which actually do the counting are both connected as toggle flip-flops. Hence, they change state whenever the clock input line has a "1" to "0" transition. FF 2 changes state with every output of OS 2 in the pulse generating logic, FF 3 changes state as a function of the state of FF 2 and the control flip-flop.

UNCLASSIFIED

UNCLASSIFIED
CONFIDENTIAL

(a) GATES

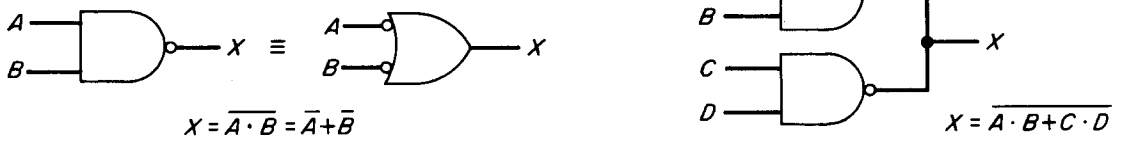

(b) SE 124 G FLIP-FLOP

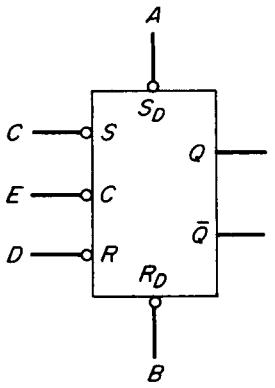

TRUTH TABLE					
A	B	C	D	E	Q $\bar{Q}$
1	1	X	X	0	NO CHANGE
0	1	X	X	0	1 0
1	0	X	X	0	0 1
0	0	X	X	0	NOTE 1
X	X	1	1	1	NO CHANGE
1	1	0	1	1	1 0
1	1	1	0	1	0 1
1	1	0	0	1	NOTE 2

1. BOTH Q AND $\bar{Q}$ ARE ONE UNTIL EITHER S_D OR R_D RISES
2. Q AND $\bar{Q}$ ARE INDETERMINANT
3. E IS "ONE" ON A HIGH TO GROUND TRANSITION AND ZERO OTHERWISE

(c) *NAND* GATE FLIP-FLOP

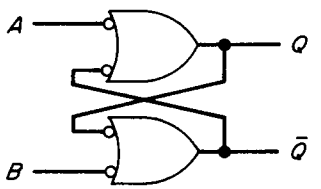

TRUTH TABLE			
A	B	Q	$\bar{Q}$
0	0	1	1
0	1	1	0
1	1	NO CHANGE	
1	0	0	1

(d) SE 160 G MONOSTABLE

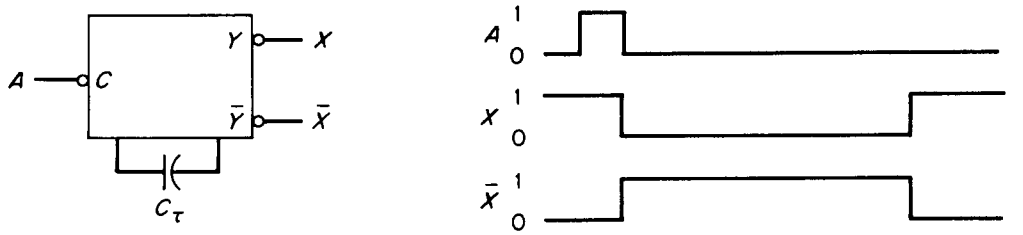

Fig. 4. Logic characteristics

UNCLASSIFIED
CONFIDENTIAL

UNCLASSIFIED

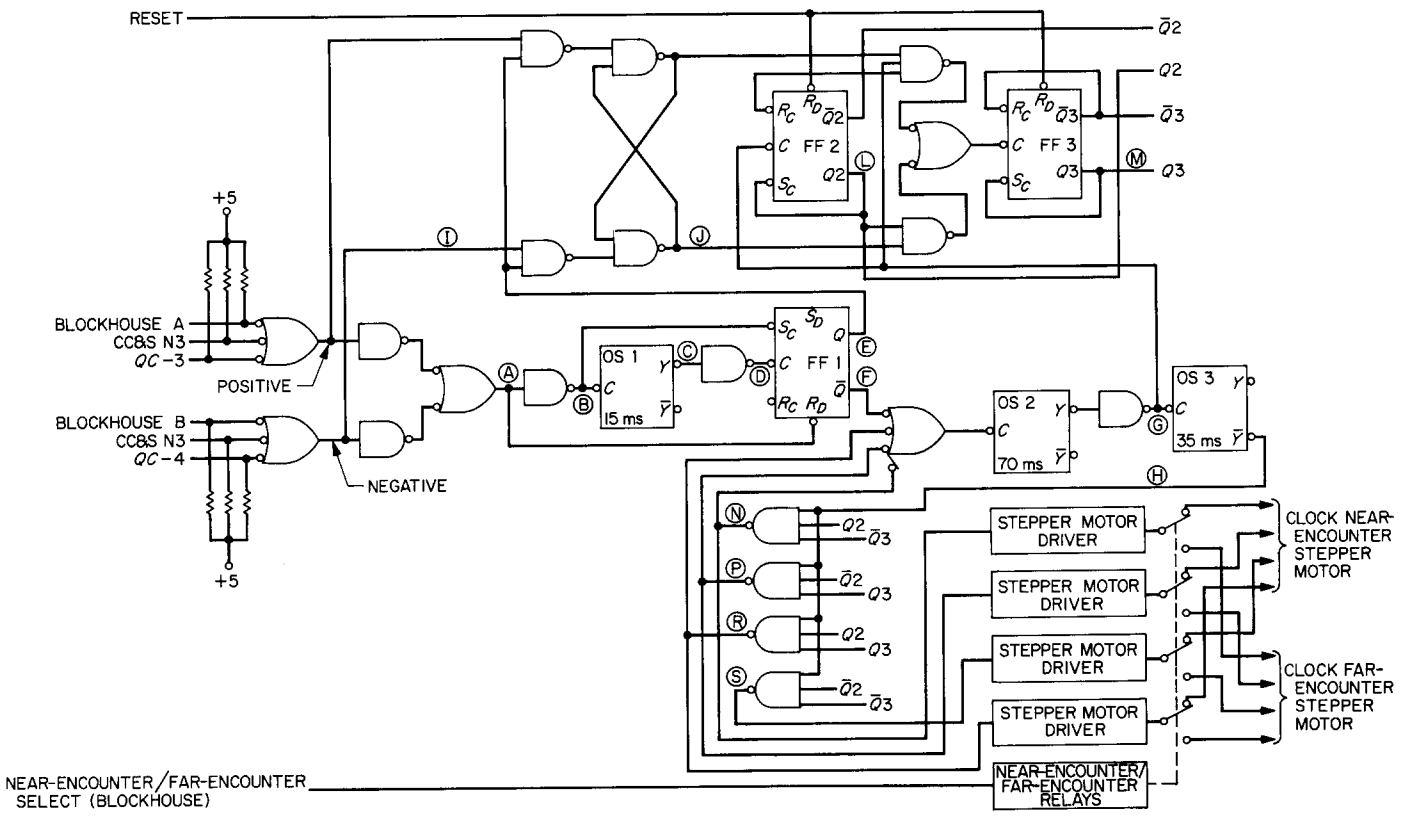

Fig. 5. Logic diagram, stepper motor drive electronics (clock)

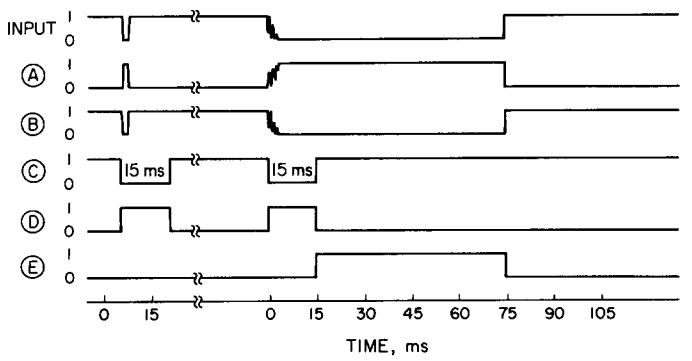

Fig. 6. Timing diagram, command delay circuit

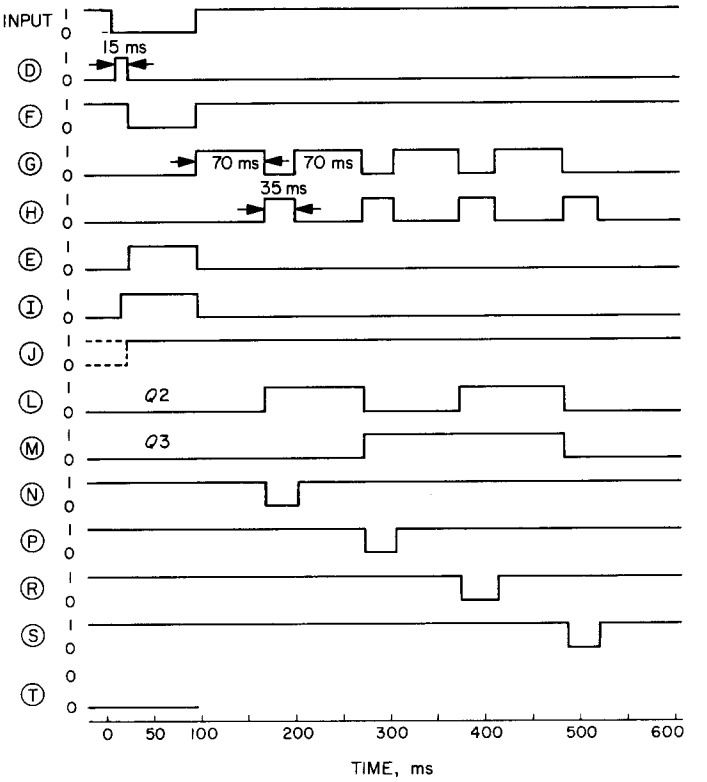

Fig. 7. Timing diagram, pulse generating logic and counting logic

UNCLASSIFIED

UNCLASSIFIED CONFIDENTIAL

The rest state of the counter is with both flip-flops reset.

Input pulse No.	Sequence 1		Sequence 2		
	Q2	Q3	Q2	Q3	
0	0	0	0	0	
1	1	0	1	1	Rest state
2	0	1	0	1	
3	1	1	1	1	
4	0	0	0	0	

A reset line is included in the logic to set FF 2 and 3 into the reset. This reset line is energized (grounded) both by power turn on (or transients) and by a DC25 command. The remainder of the logic in the stepper motor drive electronics automatically assumes the correct quiescent condition.

Stepper motor drivers. The stepper motor drivers are connected to the same counter-controlled gates which feed the output of OS 3 back into OS 2. The stepper motor can be rotated 90 deg by energizing the correct winding. The four driver circuits are energized with the proper sequence to command one complete stepper motor revolution in either a CW or CCW direction. A schematic of a stepper motor driver (all four are identical) is shown in Fig. 8.

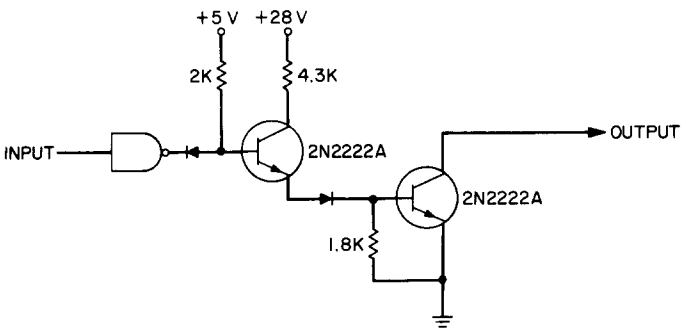

Fig. 8. Stepper motor driver schematic

The outputs of the stepper motor drivers are connected to either the far-encounter (FE) or near-encounter (NE) stepper motors through the indicated relays. These relays are energized through a blockhouse line; their unenergized (flight) condition connects the stepper motor drivers to the NE references.

c. Scan platform servo amplifiers

System description. The scan platform servo amplifiers have been designed to condition signals either from a reference source or a planet sensor to drive the platform actuator. The servo electronics consist of the clock and cone axes amplifiers. The two channels of amplifiers are identical with the exception of certain voltage gains (Fig. 9).

The actuator drives the platform in two modes. With the contact of SW 1 in position A, the servo loop is closed by the gimbal feedback potentiometer and the system performs as a position servo. With the contact in position B, the loop is closed by the far encounter planet sensor (FEPS). SW 2 grounds the modulator input to disable the platform only during the ground test.

The operating conditions include an environmental temperature range of -10 to $+75°C$ and a supply voltage variation of $\pm 15\%$ for type-approval test and $\pm 5\%$ for the flight-acceptance test.

General system design considerations. The interference between two channels may be minimized by proper shielding and packaging techniques.

The primary cause of the interference in the system is due to coupling through the common power supply. It is necessary to keep the cable length short and the supply source impedance low to avoid channel interference and local instability in emitter follower circuitry. The preamplifier input signal line must be protected from severe noise pickup. This may be caused by an input cable encircling the magnetic field or by the ground loop current (Fig. 10). The total amplifier voltage gain in the potentiometer mode is identical for both channels. For the FEPS mode, the loop gains are set differently and are adjusted at the control amplifier stage.

The integrated circuit operational amplifier μA709 has been used for each amplifier stage because of its low drift, small package size, and high reliability characteristics. All integrated circuits are provided with overvoltage and short-circuit protection. The complementary circuit design approach has been used wherever desirable to minimize drift and disturbance sensitivity.

Input considerations. In the potentiometer mode, when the gimbal potentiometer closes the loop, the source impedance seen by the amplifier input circuit varies from 0 to 750 Ω. High and balanced input impedance of the preamplifier keeps the potentiometer loading below 0.05% and loading unbalance practically negligible (Fig. 10).

UNCLASSIFIED CONFIDENTIAL

UNCLASSIFIED

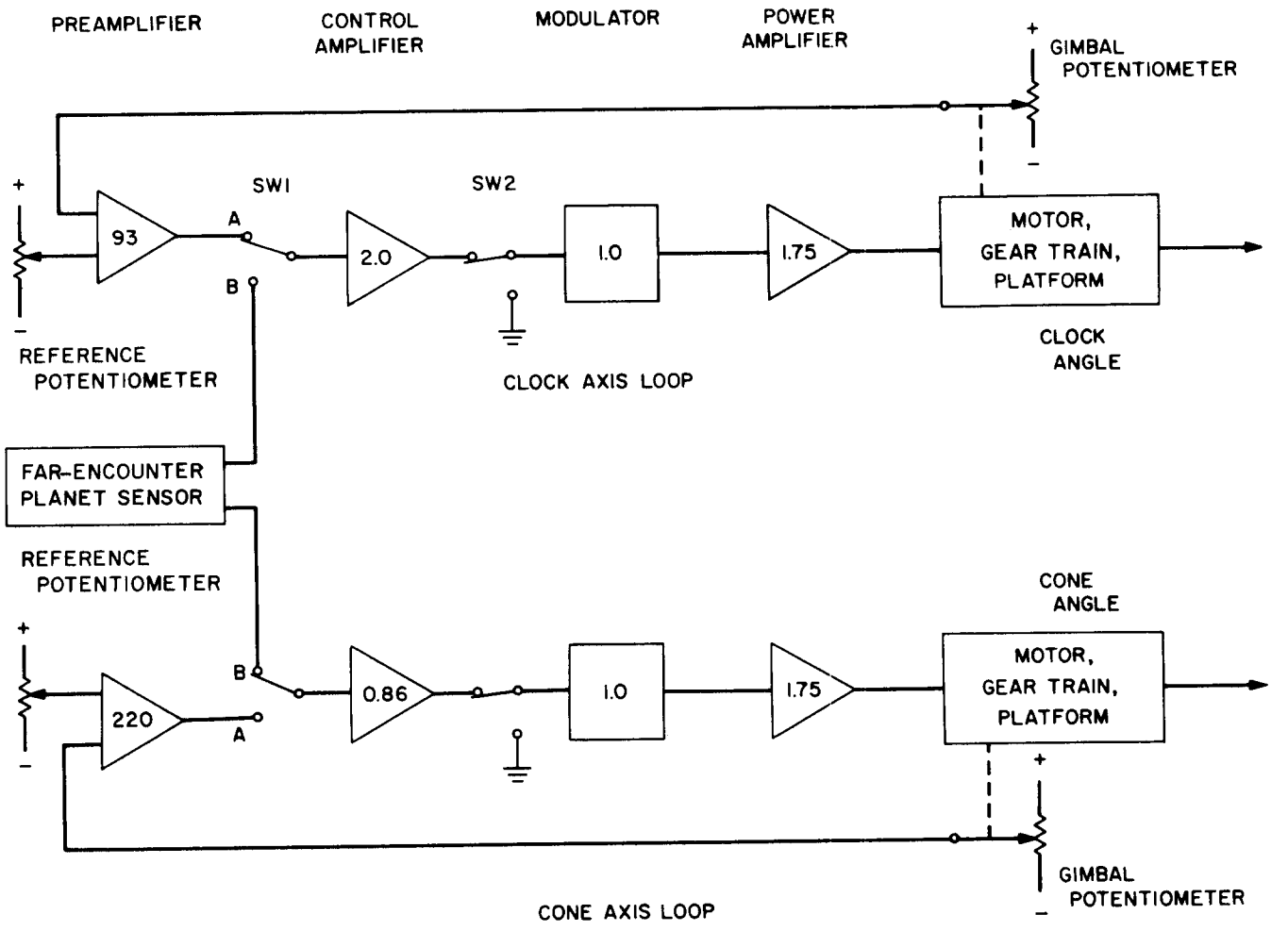

Fig. 9. System block diagram

UNCLASSIFIED

UNCLASSIFIED

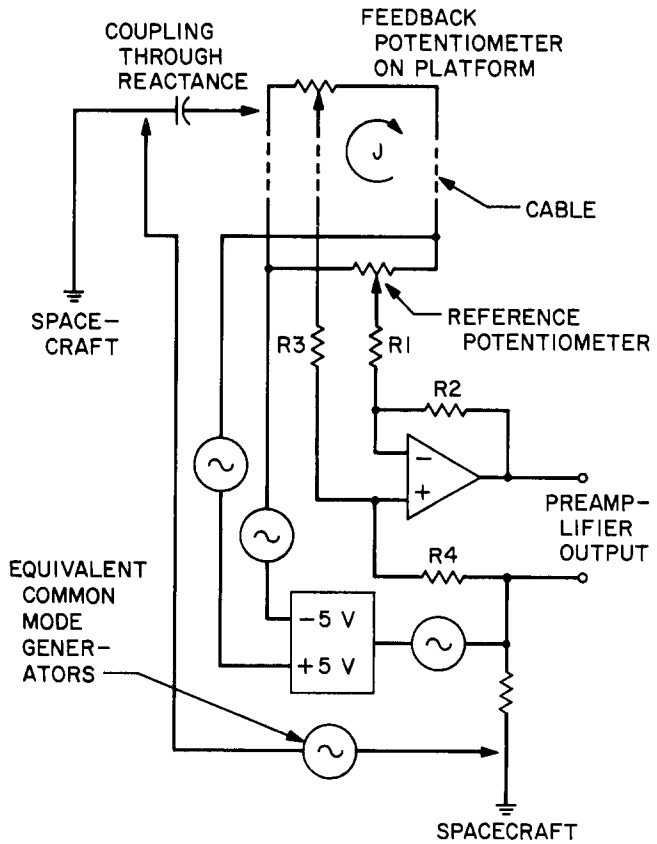

Fig. 10. Equivalent disturbance generators at input section

The two potentiometers are connected to ±5 V-supply without ground reference to minimize the effects of power supply variation (Fig. 10). At any corresponding angular positions on the potentiometers, the error voltage is a function of the potentiometer resolution, linearity, and unequal loading by the preamplifier. The system has been designed to be sufficiently insensitive to these factors. The control signal from the FEPS has already been amplified and the signal is directly fed into the control amplifier input.

Output considerations. The power amplifier operates in the Class B mode for efficiency. For the square wave drive, and when the load time constant is small, the maximum loading occurs at the trailing edge of the square wave where the load current is limited only by the motor control winding resistance. The tuning capacitor is effective only at the fundamental frequency of the square wave. When the two servo channels slew simultaneously, it is desirable to arrange such that the two motors are driven 180 deg out of phase electrically to minimize the unbalanced loading on the power supply.

Circuit Descriptions.

Preamplifier. The preamplifier is employed to provide a large voltage gain when the control loop is closed by the potentiometers (Figs. 9 and 11). In order to minimize the common mode disturbance, a differential input stage has been used to sum the reference and feedback signals. The common mode rejection ratio is limited by the intrinsic characteristics of the μA709 and is approximately 70 dB.

The two gains of the amplifier (the positive and the negative gains) are kept close to each other (±0.03%) to minimize the common mode gain. The negative gain is given by the ratio $R2/R1$ while the positive gain is given by

$$G_p = \frac{R4}{R3 + R4}\left(1 + \frac{R2}{R1}\right)$$

Requiring equal input resistance and voltage gain yields, $R1 = R3$ and $R2/R1 = R4/R3$. The resistors $R3$ and $R4$ form a simple voltage divider and are placed outside of the amplifier feedback loop.

The gain accuracy and gain stability are affected by several factors such as resistor tolerances, temperature coefficients, source resistance and finite loop gain. The maximum gain deviation is kept within the range of +3 and −4% under all conditions.

Assuming the minimum forward gain for μA709, over 40 dB of feedback are provided for the highest closed loop gain.

The maximum offset voltage referred to the input is approximately ±8.5 mV. The voltage drift over the temperature range of 85 deg will be approximately ±450 μV.

Control amplifier. The control amplifier provides a proper voltage gain between the preamplifier or FEPS and the power amplifier. The resistance–capacitance time constant in the feedback network provides a lag compensation in the control loop.

Modulator. The modulator provides a full-wave modulation of the 400-Hz carrier with the output from the control amplifier. The collector base drive is used to minimize the offset voltage in the on-mode. The modulated signal is fed into the power amplifier through a coupling transformer.

UNCLASSIFIED CONFIDENTIAL

Power amplifier. The clock and cone power amplifiers are identical. The power amplifier receives a differential signal from the modulator and drives the control windings (parallel) of the servo motor. The amplifier is provided with two feedback loops. The minor loop is to keep the forward gain constant and to provide a low drive impedance for the output driver stage. The over-all feedback determines the stage gain. The scan platform servo electronics breadboard is shown in Fig. 12.

D. Engineering Mechanics

1. Introduction

The scope of the Engineering Mechanics activities as part of the *Mariner* Mars 1969 Project has been described in SPS 37-41 and -42, Vols. II (Confidential) and VI. This report contains a current description of the spacecraft structure subsystems and the spacecraft assembly, handling and shipping equipment (AHSE). A brief description, together with results, of the torque required to twist the scan platform cabling bundle is presented. Some current results of work in the applied mechanics area are described, covering structural design analysis, separation dynamics analysis, and the structural analysis model (SAM) testing. Results of a materials engineering investigation of optical coatings for the quartz TV lens are given and also the results of electrical continuity evaluations of Anodic-coated magnesium alloy are presented.

2. Structure Subsystem

The *Mariner* Mars 1969 spacecraft structural design is essentially completed. A description of the structure's subelements is given in the following paragraphs.

a. Spacecraft adapter. The spacecraft adapter attaches the spacecraft to the forward structure (*Centaur* adapter) of the *Atlas/Centaur* boost vehicle, and positions the spacecraft base approximately 21 in. above the *Centaur* adapter forward flange. The spacecraft adapter is a 52-in.-diameter by 21-in.-high cylinder composed of the following main elements:

(1) The lower flange, made of a rolled aluminum angle section, carries the bolt pattern which allows attachment of the spacecraft adapter to the *Centaur* adapter.

(2) The skin, made of 0.025-in. aluminum sheet stabilized by vertical hat sections, and forming a cylinder approximately 52 in. in diameter by 21 in. high, provides the shear and torsional stiffness required of the adapter.

(3) The eight vertical longerons, machined from aluminum bar, provide rigid points for attachment of the eight spacecraft feet to the adapter, and smoothly deliver the concentrated spacecraft attach loads into the shell structure of the adapter.

(4) The top ring, a rolled aluminum channel section, stabilizes the top of the cylindrical skin and longerons, and provides a convenient mounting surface for miscellaneous bracketry.

b. Basic octagonal structure. The octagonal structure (Fig. 13) is the central body of the spacecraft, providing a cavity into which the electronics are mounted and acting as a rigid frame to which the scan platform, solar panels, antennas, and miscellaneous equipment are mounted. The octagonal structure, approximately 50 in. across the flats and 18 in. high, is composed of the following elements:

(1) The lower ring, a single machined part approximately 1 in. thick and 50 in. across the flats, forming a 1-in. by 4-in. channel section octagonal ring of ZK60A-T5 magnesium. This ring machining contains the eight wedge-shaped feet which permit clamping the spacecraft to the adapter via a tension band and notched shoes.

(2) The eight vertical longerons, machined 2-in. wide by 4-in. deep I-beams of ZK60A-T5 magnesium, space the upper and lower rings apart, provide lugs on one surface for the attachment of internal spacecraft truss work, and also provide an attachment flange for the mounting of shear panels to the octagon's faces.

(3) The upper ring, a machined part similar to the lower ring but with integral stabilizing spokes, serves to close the octagonal structure and provides mounting surfaces for celestial sensors, antennas, solar panels, the scan platform support structure, and miscellaneous bracketry.

(4) The scan platform support structure, a structurally redundant truss of 1-in. diameter swaged aluminum tubing, provides mounting points and roll axis bearings for the 130-lb scan platform, carrier of all the planet oriented instruments for the *Mariner* Mars 1969 mission.

(5) The superstructure, a nonredundant truss of swaged aluminum tubing, provides support for the high-gain antenna, pointing it in a fixed direction for proper communication with earth in the later stages of the spacecraft mission.

UNCLASSIFIED

UNCLASSIFIED
CONFIDENTIAL

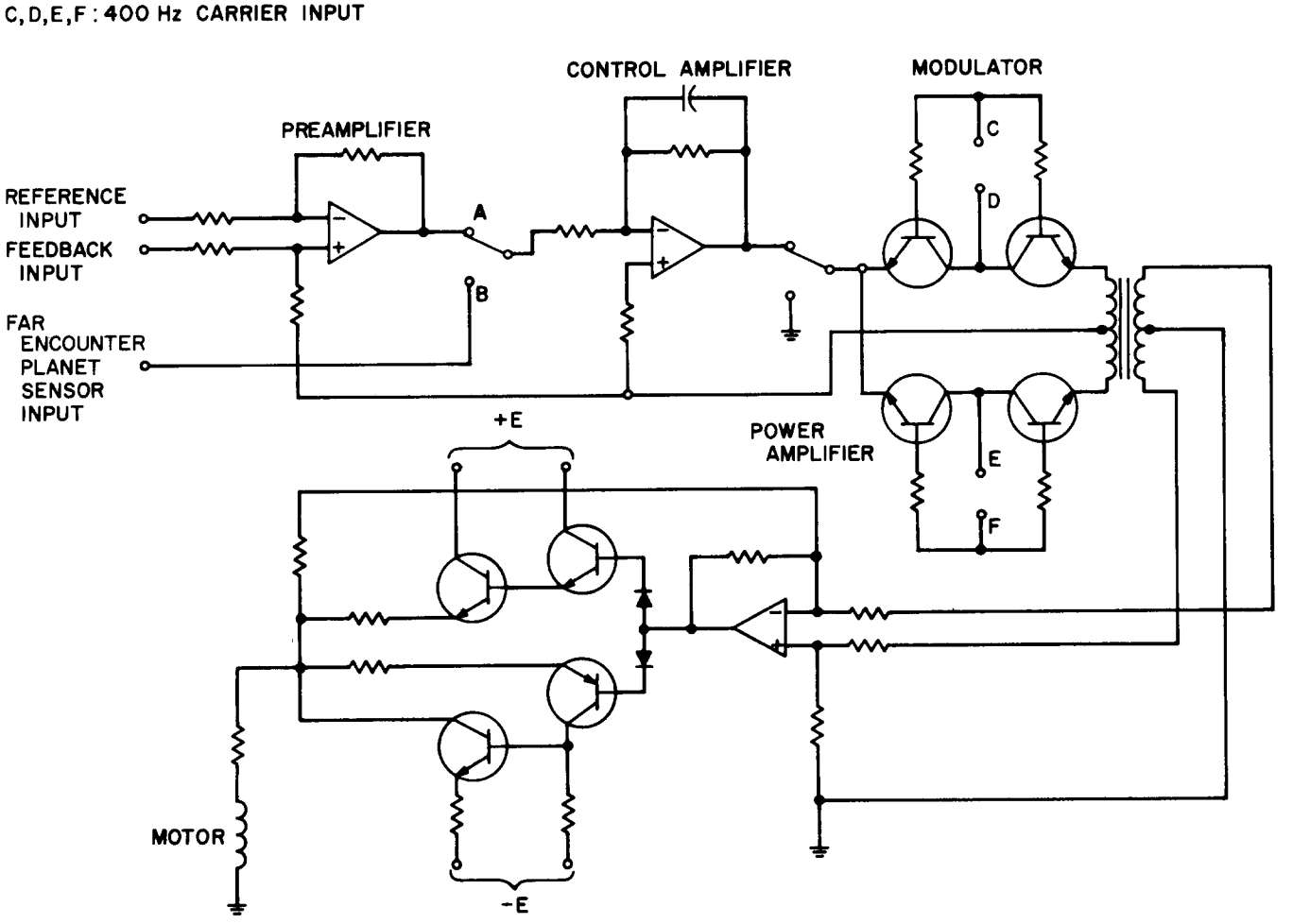

Fig. 11. Simplified typical amplifier channel

UNCLASSIFIED
CONFIDENTIAL

UNCLASSIFIED
CONFIDENTIAL

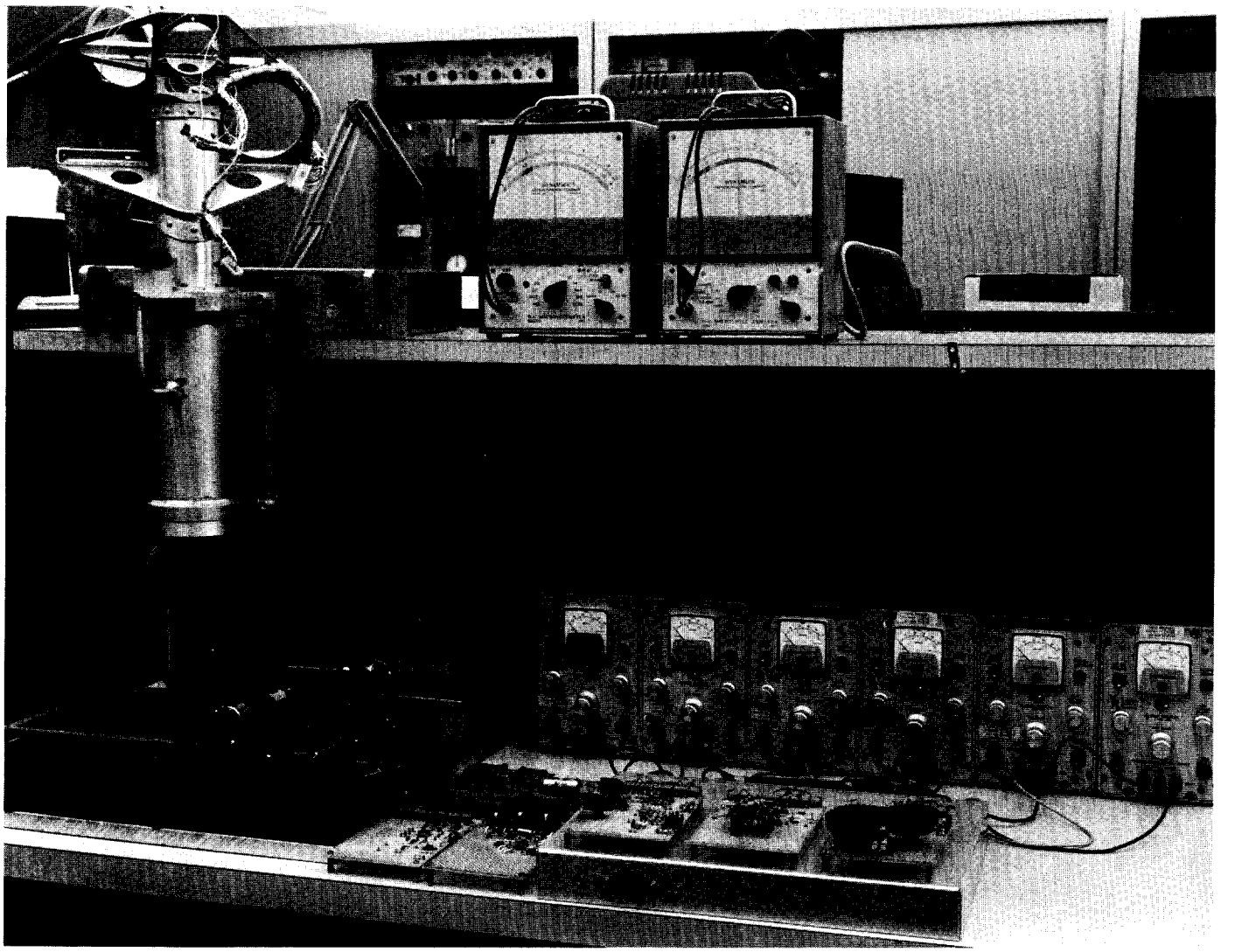

Fig. 12. Scan platform servo electronics breadboard

UNCLASSIFIED
CONFIDENTIAL

UNCLASSIFIED
CONFIDENTIAL

c. Solar panels. Each of the four solar panels on the spacecraft is approximately 3 by 7 ft. Bonded to the surface of each panel are solar cells and electrical wiring to power the spacecraft. The four panels are mounted to the spacecraft upper ring by hinged joints and are folded up to form a box 3 by 7 ft high. The tips of the panels are latched together through short spring-dashpot struts which quiet the solar panel resonances during boost vibration and permit a lightweight structure to survive the boost environment. Each solar panel structure weighs approximately 0.5 lb/ft^2 and is composed of the following main elements:

Back spars. The two back spars, made of 0.020-in. aluminum sheet formed as a 2.0- by 2.5-in. capped hat section, run vertically the length of the panel and provide it with out-of-plane bending stiffness. All loads are fed out of the panel through these spars via their hinged attachment to the octagon.

Intercostals. The intercostals, made of 20-mil aluminum, are formed as channels or box sections dependent upon their location. The intercostals tie the two spars together at the tip and base of the panel. The tip intercostal provides attachment fittings for the damped links and associated latching.

Cross braces. The cross braces, made of 20-mil aluminum formed as channel sections, tie the two spars together at their upper and lower caps, thereby providing shear stiffness and torsional stiffness to the composite spar–intercostal assembly.

Panel substrate. The panel substrate is made of 5-mil corrugated aluminum foil capped on one side with a 5-mil face skin (to which the solar cells are bonded). The corrugations are 3 ft long and lay across the spars, thereby providing no bending stiffness to augment that of the spars, but instead loading the spars in bending when the corrugations are loaded by the mass of the cells.

d. High-gain antenna structure. The high-gain antenna structure is composed of the following elements:

Parabolic reflector. A parabolic reflector 40 in. in diameter which beams the radio waves to earth. This reflector is basically a 0.5-in. thick honeycomb sandwich parabolic shell utilizing 4-mil aluminum face skins, 2-mil film adhesive bond lines, and 0.7-mil by 0.25 in. cell honeycomb core. The parabolic shell is supported by a ring beam 0.75 in. thick by 4 in. wide with a mean diameter of 20 in., the ring beam being of honeycomb construction similar to the parabolic shell.

Feed support truss. A feed support truss which locates the antenna feed in the proper position to illuminate the parabolic reflector. This truss is a bonded assembly made of molded 20-mil wall unidirectional fiberglass tubing and machined lexan end fittings. The base of the truss bolts to inserts in the face of the parabolic reflector and the top of the truss provides studs for attachment of the feed.

e. Low-gain antenna structure. The low-gain antenna structure serves the dual functions of being a circular waveguide and the support for the antenna's radiating aperture. The structure is simply a 25-mil wall, 4-in. diameter aluminum tube 7.7 ft long supported by two spring-dashpot struts and pin-jointed at its base. The tube provides attach points for miscellaneous bracketry on its exterior and mounts mode shaping antenna elements on its interior.

3. Assembly, Handling, and Shipping Equipment

The philosophy followed for the *Mariner* Mars 1969 assembly, handling, and shipping equipment (AHSE) is wherever possible to use the equipment utilized in *Mariner* Mars 1964 and *Mariner* Venus 67; to modify and use this equipment if necessary and possible; and, where these approaches are impossible, to procure new equipment.

The AHSE concept for *Mariner* Mars 1969 is primarily the same as that used in the preceding *Mariners*. The spacecraft is mounted on a universal ring (Fig. 14) from the beginning of octagon structure assembly until mating on the spacecraft adapter prior to encapsulation, except for tests requiring removal from the universal ring. The universal ring mounts on the low-level positioner (Fig. 15), which is used to orient the spacecraft as required during assembly and systems testing. While the spacecraft is on the universal ring, it is lifted by means of the universal ring. When the spacecraft is removed from the universal ring, the lift points are four brackets which bolt onto longerons on the octagon.

The spacecraft is protected by a metal canister during storage and shipment. The canister bolts to the universal ring. Purge gas will be introduced into the interior of the canister to provide a dry atmosphere during storage and shipment. During idle periods, the spacecraft is stored on a universal ring either on a service dolly (Fig. 16) or on a transport trailer (Fig. 14) when not on the low-level positioner. The solar panels are not mounted on the spacecraft for most testing of the spacecraft. When the solar panels are not mounted on the spacecraft, the attitude control gas system is supported on frames.

UNCLASSIFIED
CONFIDENTIAL

UNCLASSIFIED
CONFIDENTIAL

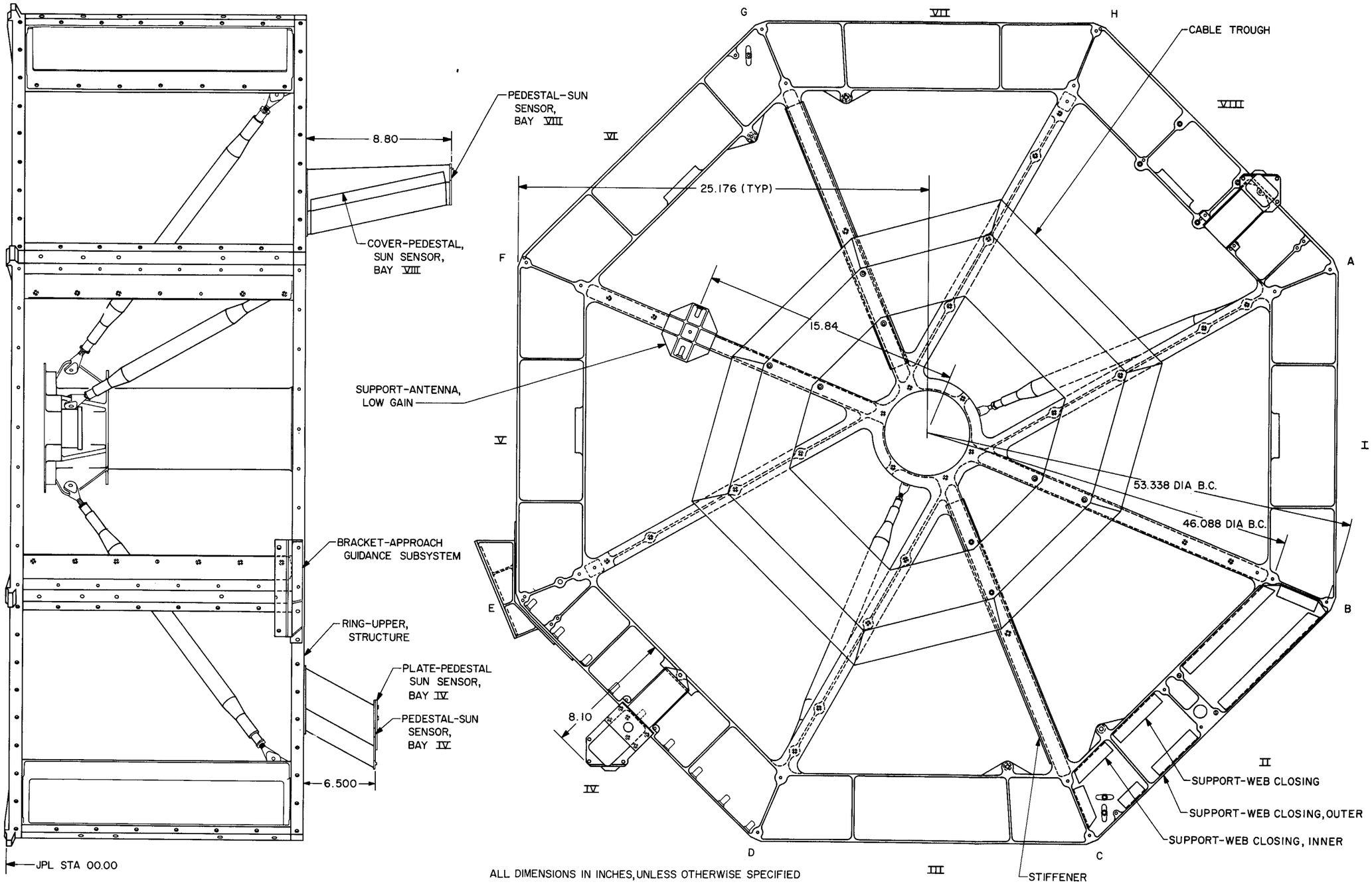

Fig. 13. Structure subsystem description of octagon

UNCLASSIFIED
CONFIDENTIAL

UNCLASSIFIED
CONFIDENTIAL

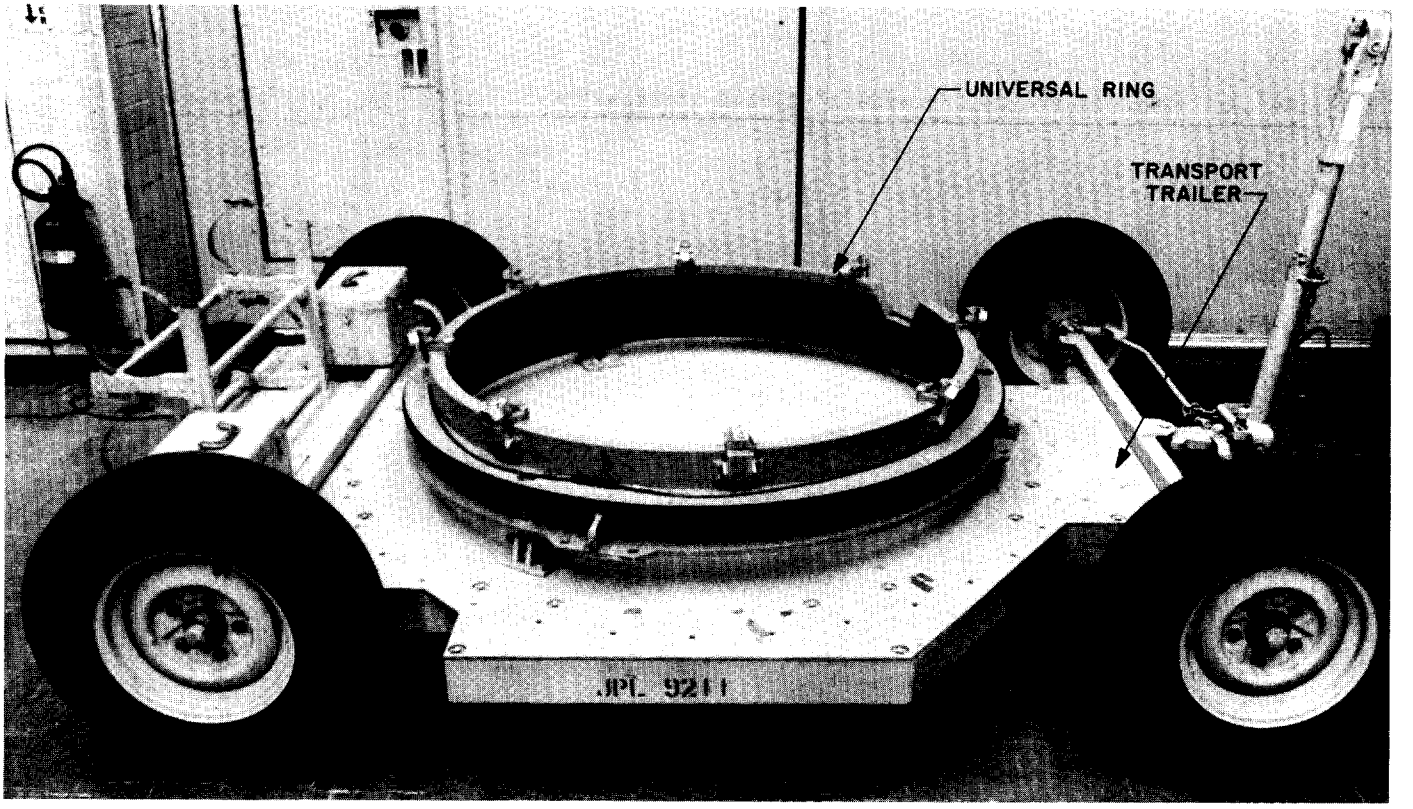

Fig. 14. Universal ring and transport trailer

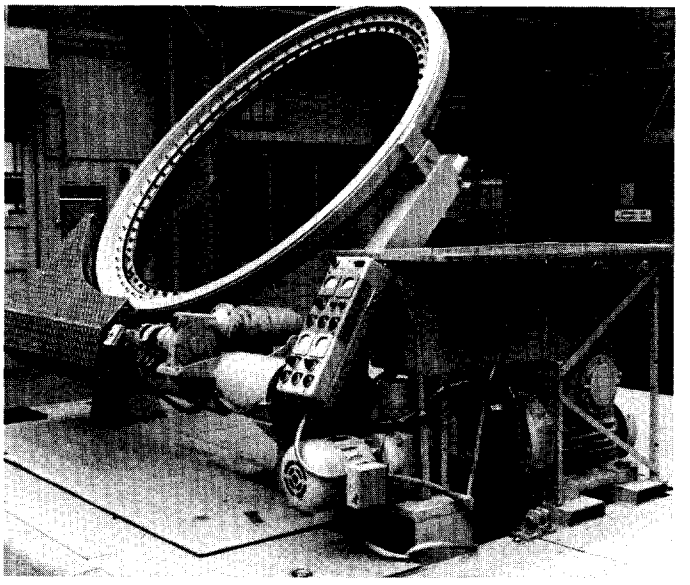

Fig. 15. Low-level positioner

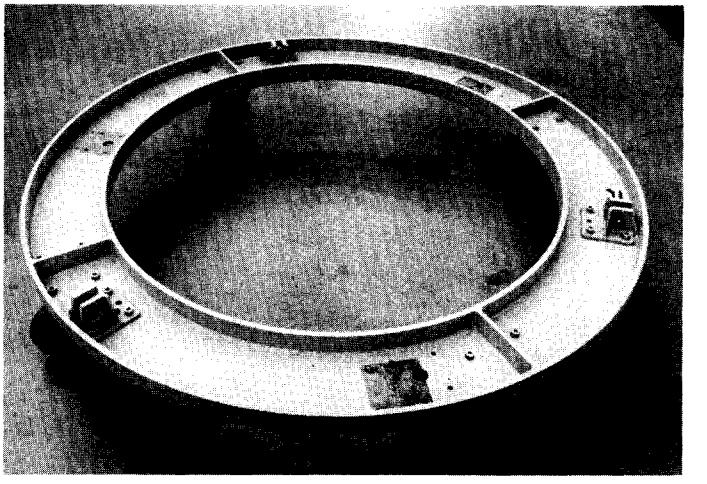

Fig. 16. Service dolly

UNCLASSIFIED
CONFIDENTIAL

UNCLASSIFIED
CONFIDENTIAL

The spacecraft is transported on a universal ring mounted on the transport trailer. For spacecraft movement between installations, the transporter will be shipped in a van (Fig. 17). To permit the spacecraft to fit in the van for shipment, the solar panels are replaced by gas frames, the low-gain antenna is removed, and a shortened protective canister is used.

The *Mariner* Mars 1969 differs from the *Mariner* Mars 1964 spacecraft by: (1) a large diameter dimensional envelope due to the Canopus tracker head, the approach guidance experiment, and the propulsion subsystem cover; (2) the 11-in. longer solar panels which in turn result in a longer low-gain antenna; (3) the larger scan platform which extends further below the spacecraft separation plane; (4) the greater weight of *Mariner* Mars 1969; (5) transfer of the upper spacecraft adapter from launch vehicle to spacecraft system cognizance; (6) the use of the *Centaur* launch vehicle; (7) the change of the high-gain antenna from elliptical to circular outline; (8) repackaging of the science and attitude control electronics; and (9) changing the mounting method of the propulsion subsystem.

These nine areas of difference between *Mariner* Mars 1964 and *Mariner* Mars 1969 affect the AHSE in the following ways:

The larger diameter required to clear all hardware means a larger protection can is necessary. The can will require a transition section extending from the present mounting surface on the universal ring for support. Since the diameter of the universal ring at the lifting points is less than the diameter of the protective can, there must be provision for passing the four sling cables through the can envelope. The lengthened solar panels require that new solar panel handling frames be procured. The new

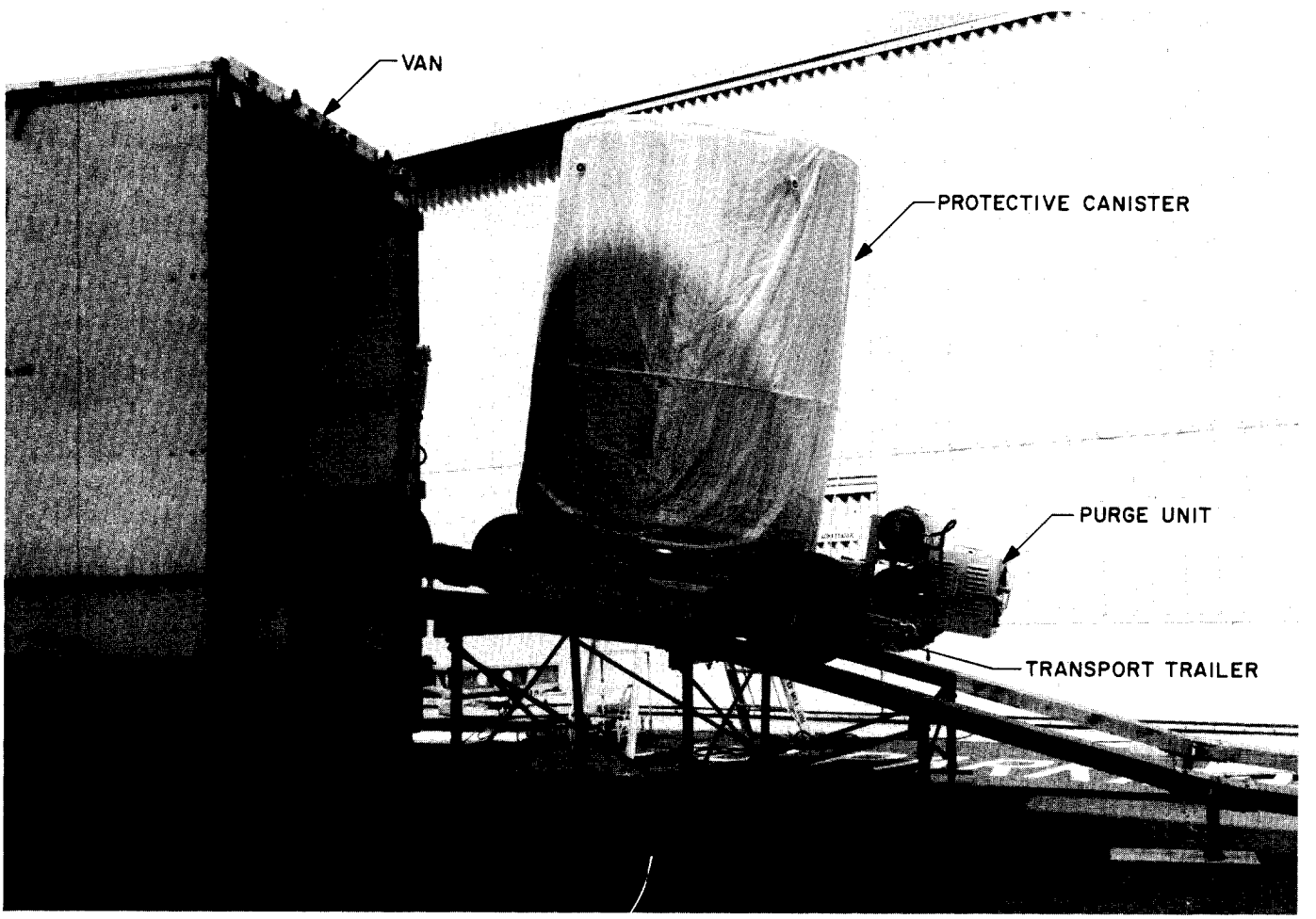

Fig. 17. Loading spacecraft into van

UNCLASSIFIED
CONFIDENTIAL

UNCLASSIFIED
CONFIDENTIAL

frames require minor modifications to the solar panel transport trailer cradles. The longer low-gain antenna requires an extension to the present low-gain antenna shipping containers. In addition, the spacecraft protective cans must be lengthened. Similarly, the sling lengths must be increased.

The larger scan platform extends below the universal ring and even below the plane of the bed of the transport trailer. Therefore, a spacer is fitted to the bottom of the universal ring during storage and transport of the spacecraft. The spacer encloses the scan platform and will mount on the transport trailer or the service dolly. The additional weight requires that the strength of all present AHSE be evaluated to provide the desired 3.5 factor of safety.

The transfer of cognizance for the adapter and separation results in the inclusion of spacecraft-adapter mating hardware and V-band installation tools and instrumentation. In addition, a V-band tension monitor must be provided for the blockhouse launch complex equipment.

The *Centaur* launch vehicle brings a new set of GSE with which the spacecraft must be integrated. This includes the *Surveyor* transport trailer and *Centaur* shroud-spacecraft lift fixture.

The new high-gain antenna requires a new shipping container and handling frame.

The repackaged electronic assemblies require new handling frames for handling and shipping, and the modification of the electronic assembly swingout tool to reach into the octagon to attach to the new configuration assemblies.

The revised mounting of the propulsion subsystem requires a new fixture fitting into Bay II for mounting the spacecraft on the Z-axis weight and CG stand, and a new fixture for determining the weight and CG of the propulsion subsystem.

4. Science Platform Cabling

A mock-up of the science platform basic tubular support members was constructed for studies of cable routing and the effects on cables during clock and cone slew of the science platform.

The science platform cabling was studied and tested with the use of a mock-up constructed of transparent plastic. This mock-up was of the structural tubing which

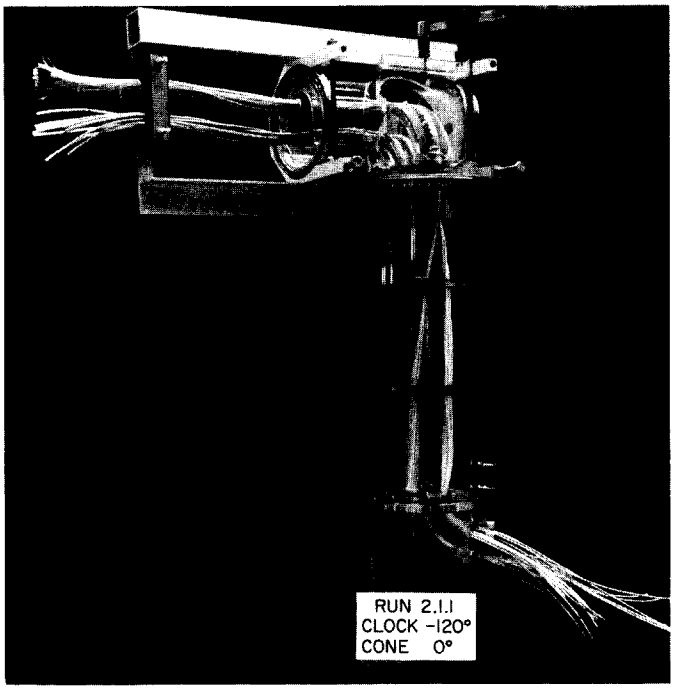

Fig. 18. Scan platform articulation test mock-up

forms the mechanical articulating members. The cables were divided into three separate bundles: power, signal, and pyro, and they were installed with supporting separators, as shown in Fig. 18. Tests were then performed to determine the torque required, due to the resistance of the cables to twisting, to move the scan platform into various positions. These tests also gave the opportunity to observe the effects on the cable during platform motion. At the start of the test, the cone angle was adjusted for a zero torque reading. Results of the tests indicated that torques were well within the capabilities of the scan actuating motors. The worst-case torque in the clock angle was 70 in.-oz at -120 deg with cone angle at 0 deg. The worst-case torque was 60 in.-oz in the cone axis with the cone angle at $+40$ deg and with the clock angle at -120 deg (Fig. 19).

The tests were accomplished at normal room ambient temperature. Torque tests in the worst-case environment (low temperature) are scheduled for a later date.

5. Applied Mechanics

The content of the structures and dynamics effort can be divided into three fundamental regimes: direct analytical support of the design development, dynamic analysis of the launch vehicle–spacecraft separation event, and static and dynamic testing of the spacecraft or components thereof.

UNCLASSIFIED
CONFIDENTIAL

UNCLASSIFIED
CONFIDENTIAL

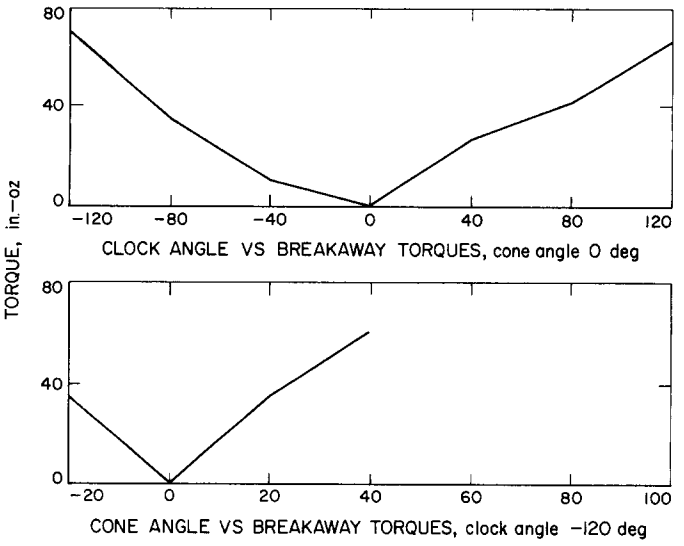

Fig. 19. Torque required to position scan platform

a. Structural design analysis. The primary effort over the last period has been the analytical support of the design effort for the major *Mariner* Mars 1969 structural elements. This support has emphasized the determination of critical loads imposed upon major spacecraft components as a result of the estimated static and vibration environments applied to the spacecraft. The stress analysis effort utilizing either the above mentioned loads, or previous estimates, has been concentrated on those areas in which a design change required to ensure structural integrity would be most detrimental to the previously adopted schedules.

This analytical effort, while primarily directed to support of engineering mechanics subsystems, required interaction with, and analytical design support of, all subsystems including the scientific instruments.

Spacecraft structure. Structures and dynamics support of the program was increased as the design progressed. During the last period all of the major structural components received at least a preliminary analysis.

The majority of these analyses were performed using the recently developed SAMIS[3] computer program. This program has the capability of simulating the structure by an array of both one- and two-dimensional elastic elements, and of generating natural frequencies, mode shapes, and internal loadings on each elastic element. The frequencies and mode shapes of these components were combined, using the Modal Combination[4] Program. The results of this modal analysis were compared to the experimental results of the SAM modal testing. Considering the mock-up nature of the test article and the preliminary nature of the analysis, the correlation was reasonable.

Adapter. The analysis of the adapter was essentially twofold. One objective was to ensure that the strength of the adapter was greater than the previously accepted maximum interface load. The second objective was to determine how the flexibility of the adapter affected the dynamic response of the spacecraft.

The strength analysis of the adapter was performed, using standard "elementary" techniques. Buckling at less than ultimate load was not permitted. The flexibility of the adapter was determined using the SAMIS computer program. The results of this analysis were compared to the experimental results determined during the SAM static tests. Initially the correlation was poor, and additional static testing and more analytical work was accomplished. Results indicated that the computer solution was more sensitive than expected to certain geometric properties used in the structural idealization. This phenomenon is still being investigated.

Scan platform. Much effort has been expended on the scan platform structure, since it is both an important and complex portion of the spacecraft. The analysis which results in natural frequencies, normal mode shapes, and internal loads of the scan platform when installed in the spacecraft was performed using the SAMIS computer program.

A portion of the structure, idealized for the SAMIS program is shown in Fig. 20. The circles and squares represent joints, while the connecting lines represent elastic elements. The structure was idealized as a three-dimensional combination of beam and plate elements, and the instruments idealized as point masses.

Solar panel boost dampers. The solar panel boost dampers require a different analytical approach from that of the previous examples.

The solar panel boost dampers play an important role in reducing the solar panel tip deflection due to lateral vibration excitation. Since the damping characteristics of

[3]Melosh, R. J., Diether, P. A., and Brennan, M., *Structural Analysis and Matrix Interpretive System (SAMIS) Program Report*, Technical Memorandum 33-307, Revision 1. Jet Propulsion Laboratory, Pasadena, Calif., Dec. 15, 1966.

[4]Bamford, R. M., *A Modal Combination Program for Dynamic Analysis of Structures*, Technical Memorandum 33-290. Jet Propulsion Laboratory, Pasadena, Calif., Aug. 15, 1966.

UNCLASSIFIED
CONFIDENTIAL

UNCLASSIFIED
CONFIDENTIAL

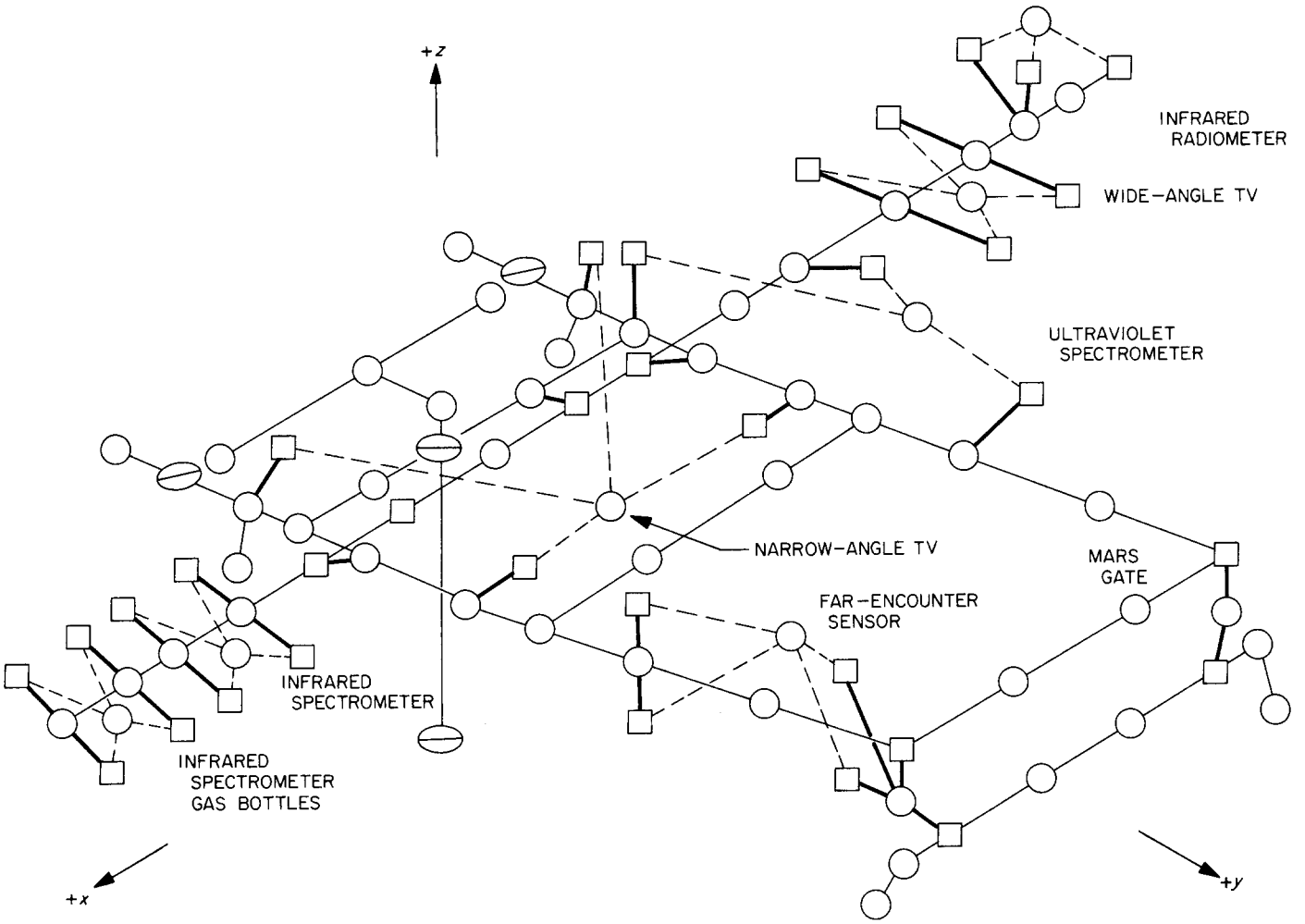

Fig. 20. Main scan platform

CONFIDENTIAL
UNCLASSIFIED

UNCLASSIFIED
CONFIDENTIAL

the dampers are nonlinear, the correct results cannot be obtained from the linear analysis for which the computer programs are developed. The damping coefficient and phase angle of a nonlinear damper are not constant, but vary with frequency. The dynamic response of the solar panel/damper structural system is obtained by iterating the damping component of the total damper force to match the amplitude at a particular frequency. The response obtained is only valid for that particular frequency. For the responses at other frequencies, the whole iterating procedure has to be repeated. It is believed that this kind of analysis will give better correlation to test results than that used on previous *Mariner* programs.

Damper characteristics which include damping force and phase angle as function of frequency and amplitude will be obtained from damper development tests now in process.

b. Separation dynamics analysis. Spacecraft separation analyses have been performed to determine the motions, absolute and relative in six degrees of freedom, of the *Mariner* Mars 1969 spacecraft and *Centaur* during the separation event.

The basic mathematical approach to the problem is a straightforward application of the Lagrange equations augmented by undetermined multipliers. The equations of motion are written in a reference frame that has fixed directions in inertial space, but that moves with the preseparation trajectory of the two bodies, e.g., the spacecraft and *Centaur*. The equations of motion are solved on the IBM 7094 computer for the accelerations which are then twice-integrated to give the velocities and displacements.

The results of the analysis indicate that the *Mariner* Mars 1969 spacecraft will nominally separate from the *Centaur* with an absolute velocity of 19.5 in./s and relative velocity of 23.6 in./s. The angular rate produced by the maximum spacecraft CG offset is 0.44 deg/sec, corresponding to pitch and yaw rates 0.30 and 0.67 deg/s, respectively. The maximum *Centaur* residual angular rate is considered to be 1 deg/s. If the direction of this residual angular rate is the same as that caused by the spacecraft CG offset, the combined angular rate will be 1.46 deg/s, corresponding to pitch and yaw rates 1.01 and 1.06 deg/s, respectively.

It is possible for each of the four springs included in the spacecraft separation system to have errors in useful stroke, precompression, rate, and alignment angle. These errors are the result of machine and/or material tolerances, which to a certain extent cannot be eliminated in the construction of the separation system. The results of each individual error are small perturbations in the spacecraft attitude and angular rate following separation. The most severe combination of the maximum errors due to spring tolerance CG offset and *Centaur* residual rate results in a total residual rate slightly in excess of the originally specified limit. Since both the error estimates and the specified limit are conservative, this problem should be readily solved.

The induced angular rates of the spacecraft due to the various spring errors about its pitch and yaw axis, as well as the vector sums of pitch and yaw rates, are listed below. It is assumed that the tolerances combine in such a manner so as to induce the maximum perturbation for the given tolerances value in the direction of angular rate caused by the spacecraft CG offset.

Item, deg/s	Pitch	Yaw	Vector sum
Separation–initiated timer	0.0084	0.01	0.013
Spring misalignment	−0.021	0.106	0.108
Spring rate	0.626	0.224	0.675
Spring stroke	0.347	0.121	0.362
Spring precompression	0.569	0.196	0.602
Arithmetic sum	1.529	0.657	1.67

Combining the angular rates caused by the spacecraft CG offset and the *Centaur* residual rate with the angular rates caused by the spring errors will give an over-all worst possible spacecraft angular rate induced by the separation. This angular rate is 3.07 deg/s, which corresponds to pitch and yaw rates 2.542 and 1.713 deg/s, respectively.

It is very unlikely that the worst possible angular rate of the spacecraft during the separation will occur, because of the random nature of the spring tolerances of the separation system. It is clear that a statistical error analysis will furnish a rational method of weighting and combining the influences of individual error sources to yield a total angular rate.

A successful spacecraft separation requires not only that the induced angular rate not exceed the recovering capability of the control system, but also that there be adequate clearance between the spacecraft scan platform

UNCLASSIFIED
CONFIDENTIAL

UNCLASSIFIED
CONFIDENTIAL

and adapter. Therefore, an analysis of the trajectory of the critical points on the scan platform and adapter during the separation is necessary. The computer program, which calculates the separation velocity and angular rate, also gives the coordinate transformation matrices which show the relative position of the spacecraft to the *Centaur*. These coordinate transformation matrices are functions of time throughout the process of the separation. Another computer program is developed to use these coordinate transformation matrices and the coordinates of the critical points on the spacecraft scan platform and adapter in order to calculate the trajectory of those critical points during the separation.

c. SAM testing. The purposes of the SAM structural developmental tests are to acquire test experience to expedite forthcoming structural test model testing and to provide a realistic basis for evaluating the analytic capability to predict spacecraft response characteristics. In static tests, influence coefficient values were obtained for the primary structure. The possibility of physical separation between the spacecraft and adapter, when clamped with the V-band assembly, was also investigated. Strain gage data were obtained on the *Mariner* Mars 1969 adapter, which provided an indication of the ability of this adapter to transfer the concentrated foot loads to a distributed load across the *Centaur* adapter interface. The strain distribution induced in the adapter when bolted to the *Centaur* adapter was checked for the estimated maximum tolerance build-up condition.

A typical static test determined influence coefficients for the isolated *Mariner* Mars 1969 adapter. Two sets of lateral deflection influence coefficient values were obtained at the four alternate feet located atop the spacecraft adapter for the special case of a rigid *Centaur* adapter mounting. The adapter was mounted to the modal test plate, as shown in Fig. 21. Dial gages were mounted against the adapter top ring at the base of alternate feet. Loads were applied at leg A by a wire line loop connected to a hydraulic jack and monitored by an in-line mounted 2000-lb capacity load cell. Deflections

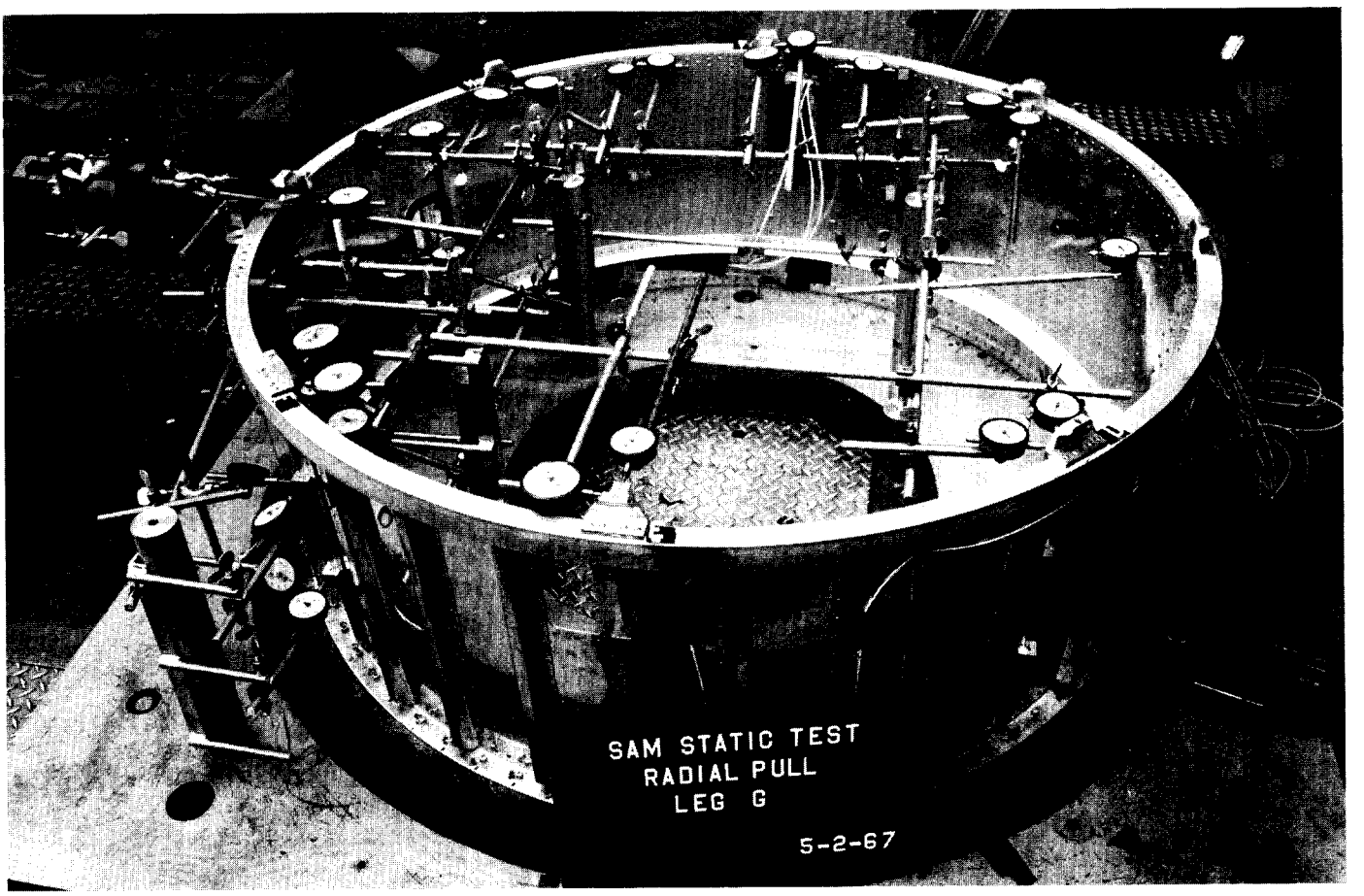

Fig. 21. Structural analysis model

UNCLASSIFIED
CONFIDENTIAL

UNCLASSIFIED
CONFIDENTIAL

were recorded from zero at approximately 250-lb load increments up to 1000 lb and then again at zero load. Two test runs for radial load and tangential loading provided an indication of data repeatability. All of the deflection data were plotted versus the applied load. These plots indicate a minimum of data scatter, an acceptable amount of permanent set, and a continuously linear increase in deflection with load. Other test configurations were: the spacecraft mounted on the *Mariner* Mars 1969 adapter with and without planetary scan platform (PSP), and spacecraft mounted on both adapters with and without PSP. Loadings were applied to these test configurations in lateral, tangential, and axial directions.

Modal tests determined the SAM primary modal frequencies, mode shapes, and structural damping in the 5- to 200-cps frequency range, both with and without the scan platform, for comparison with the *Mariner* Mars 1969 analytically predicted values. A typical modal test setup is illustrated in Fig. 22. The *Mariner* Mars 1969 adapter is bolted to the modal test plate, and the spacecraft is attached to its adapter by means of the V-band. Excitation is provided by four 25-lb force shakers which are elastically and pendulously suspended from the modal support structure.

Various combinations of shakers were required to excite clean normal modes of the test structure. Dynamic

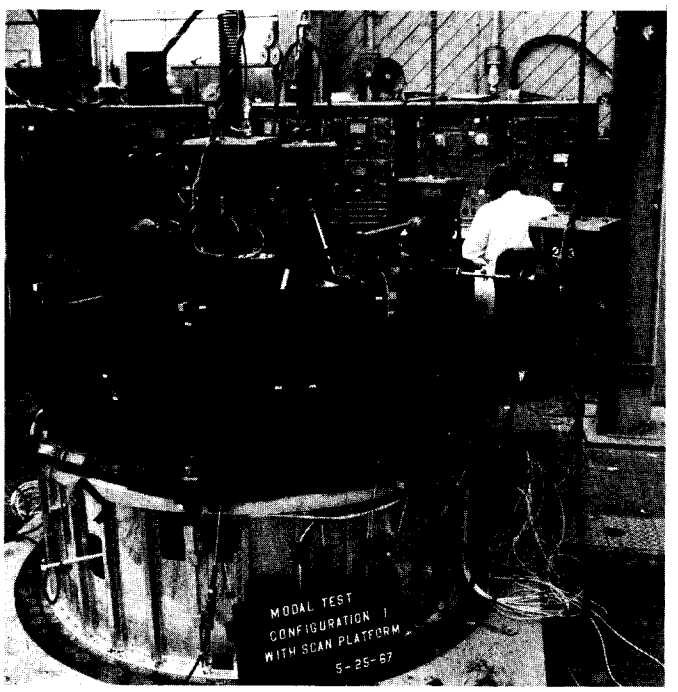

Fig. 22. Modal test configuration 1 with scan platform

mode shapes were monitored with small portable accelerometers attached to the test structure by means of double back elastic tape. Structural damping of normal modes was obtained from the logarithmic decrement of acceleration amplitude decay when excitation to the SAM terminated. Measured mode shapes have been plotted for comparison with analysis. Structural damping has been determined and is of the order of one-half of 1% of critical damping.

The types of modes measured include lateral bending, bus breathing and shear type modes, scan platform primary modes, and coupled scan platform/bus modes. Acceleration wave form in normal modes indicated a tight, linear structure which was verified by the wave form and frequency of the acceleration logarithmic decrements. Test configurations implemented to meet the basic objectives of the modal test program were the spacecraft mounted on the *Mariner* Mars 1969 adapter with and without the PSP, and spacecraft mounted on both adapters with the PSP. A total of 32 modes was recorded.

6. Materials Engineering

a. TV camera cover lens coating. The *Mariner* Mars 1969 science platform is thermally decoupled from the spacecraft bus and is in the shade during flight; thus, thermal control of the platform must be predicated on preventing the science instruments from becoming excessively cold. This is accomplished, in part, by use of a thermal insulation cover blanket which minimizes heat losses from within the platform. However, one of the science experiments, a narrow-angle TV camera, has a 9-in. diam quartz cover lens which penetrates the insulation blanket and views space. Since the thermal emittance of quartz is high, $\varepsilon > 0.80$, the lens is, in essence, equivalent to 50 in.^{2} of black emitting area. Thus, it is necessary for the optical properties of the quartz lens to be modified by coating it with a material which exhibits a low thermal emittance and, in addition, has the high visible transmittance required for operation of the camera. The initial design requirements established for the lens coating were: visible transmittance $\geqq 0.80$; thermal emittance $= 0.10$.

Initially, a brief survey was conducted to ascertain the availability of optical films for use on quartz which would exhibit the requisite properties of high visible transmittance and low thermal emittance. From this survey it was determined that several companies have commercially available proprietary coatings with optical properties approaching the design requirement. Typically, these coatings are in a similar class in that they utilize an extremely thin film of gold with a protective dielectric

UNCLASSIFIED
CONFIDENTIAL

CONFIDENTIAL UNCLASSIFIED

overcoat. Since the indication was that a coating development program would not be necessary, the task transformed into an evaluation of the commercially available optical coatings.

The evaluation of these coatings was performed utilizing the two grades of optical quality quartz which are candidates for use on the TV camera cover lens, namely Homosil or Spectrosil. All sample blanks used during tests were optically polished to a flatness within a few fringes, following which the samples were submitted to the various vendors for processing. Four vendor coatings were evaluated and the suppliers included: Libbey–Owens–Ford Glass Co., Optical Coating Laboratory, Perkin Elmer Corp. and Eastman Kodak Co.

Optical property values for the coated samples (Table 9) were determined from measurements performed at Northrop Space Laboratories.[5] The transmittance property was attained using a Cary Model 15 recording spectrometer with a tungsten lamp source. Spectral transmittance curves covering the wavelength interval of interest (4800 to 7000 Å) were generated and from these curves the average transmittance was calculated. The normal spectral reflectance (2 to 25 μ) of the coated samples was determined by standard techniques using a Perkin Elmer 13U spectrophotometer with a heated cavity attachment. A total normal emittance value was calculated from the reflectance curve of each sample.

Table 9. Optical properties of high transmittance–low emittance coatings

Vendor	Average transmittance	Calculated total emittance
Libbey–Owens–Ford Glass Co.	0.84	0.08
Optical Coatings Laboratory	0.81	0.15
Perkin Elmer Corp.	0.83	0.10
Eastman Kodak Co.	0.80	0.09

An integral part of the evaluation was the determination of the mechanical and environmental stability of the various coatings. All samples were tested for adherence, abrasion resistance, thermal shock and humidity.

Adherence. All vendor samples passed the standard adherence test performed by abruptly pulling pressure-sensitive tape from the coating surface as described in MIL-M-13508.

Abrasion and handling. All coatings meet the standard vendor certification for typical optical coatings. In brief, these tests consist of various rubbing treatments using pastes and soft cloths. In addition, an extremely severe test, as is described in JAN-F-676-F-2f, was utilized. This test consists of abrading the surface with a hard rubber tip loaded to 25 psi. The wear resistance is a function of the number of cycles until incipient damage occurs. The Libbey–Owens–Ford coating withstood two cycles, the remaining three coatings withstood one. Even the most severely abraded portion of the coatings still had acceptable optical properties.

Thermal stability and shock. The coatings can withstand temperatures well in excess of those they will encounter throughout any phase of the mission. Emittances of all vendor coatings were measured at temperatures up to 500°C. No change was noted up to 300°C. Selected Libbey–Owens–Ford samples were heated for 5 h at 400°C. After heating, there was no increase in emittance. In another test, two Libbey–Owens–Ford samples were cooled to 30°F, rapidly heated to 125°F, suddenly chilled to −100°F, and again rapidly heated to 125°F. The temperature cycling had no effect on the properties of the coating.

Humidity. Exposing the samples in a humidity chamber to an atmosphere of nearly 100% relative humidity at 100°F for 100 h resulted in visible blemishes on most samples. However, the optical properties of the Libbey–Owens–Ford and the Optical Coatings Laboratory coatings did not degrade. The emittance property of the Perkin Elmer and Eastman Kodak coatings degraded by at least 20%.

As a final requirement, the lens coating underwent semiquantitative spectrographic analysis to assure that the materials utilized would be compatible with the space environment. The analysis showed that no elements were present which were considered detrimental.

Conclusions. The initial design requirements established for the TV camera lens coating were successfully met. A rating system, devised to give weight to the more important characteristics such as optical properties, was established to rank the four individual vendor coatings which were evaluated. Based on the results briefly described herein, the Libbey–Owens–Ford coating rated the highest. This proprietary coating is designated "Hardened

[5]Srepal, V., *Mariner Mars '69 Engineering Mechanics Subsystems, TV Window Coating*, NSL66-4015-1. Nortronics, Northrop Corp., Hawthorne, Calif., Feb. 1967.

UNCLASSIFIED CONFIDENTIAL

UNCLASSIFIED
CONFIDENTIAL

IR-81E." The Libbey–Owens–Ford coating transmits in excess of 80% of the light in the wavelength band 4800 to 7000Å, and its total normal emittance is 0.08. Taking into account the small variations which occur during processing, as well as the uncertainty in measurement, the emittance of the lens should be 0.10 $\pm$0.03. Discussions with Libbey–Owens–Ford personnel indicate that the uniformity of the coating over the 9-in. diameter surface will be within 2.5%. A specification for the Libbey–Owens–Ford coating, FS502757, has been released.

b. Electrical continuity of anodic-coated magnesium alloy.

Introduction. The *Mariner* Mars 1969 spacecraft design requires the structure and electronic assemblies to be in electrical contact to provide a common ground. This requirement does not appear difficult to satisfy. However, such is not the case since the magnesium alloys constituting the major portions of the spacecraft and electronic assemblies are highly susceptible to atmospheric corrosion. Efficient utilization of these alloys requires that they be protected by coatings such as phosphate, chromate, oxide, or metallic plating. The nonmetallic coatings exhibit either poor electrical conductivity or are nonconductive; whereas the platings have emissivity values too low to satisfy temperature-control criteria.

In past spacecraft designs, acceptable but sometimes marginal, electrical conductivity was achieved by the use of the Dow-7 conversion coating. However, since Dow-7 coated magnesium parts have corroded during assembly, testing, and prelaunch storage on several occasions, a program was initiated to ascertain the feasibility of using Dow-17, a more corrosion-resistant coating than Dow-7. The Dow-17 coating affords superior corrosion resistance, but is an anodic, nonconductive coating. The approach of obtaining electrical continuity through the mechanical fasteners which join the various components of the spacecraft seemed feasible and was investigated.

Program. Magnesium alloy ZK60A-T5 plates were anodically coated with Dow-17 by a commercial coating vendor, and mechanically joined into assemblies. A typical assembly is shown in Fig. 23. Various types of fasteners were used in the assemblies to determine if the type of fastener affected the electrical continuity through the anodically coated assemblies. The types of fasteners used were Keensert inserts, Rosan washers, Rosan inserts, Press-nuts, and B-size rivets (Fig. 24).

Each plate was coated with Dow-17 on all surfaces. The fastener holes in two assemblies were drilled before the coating operation so that they were coated with Dow-17. The holes in four assemblies were drilled after

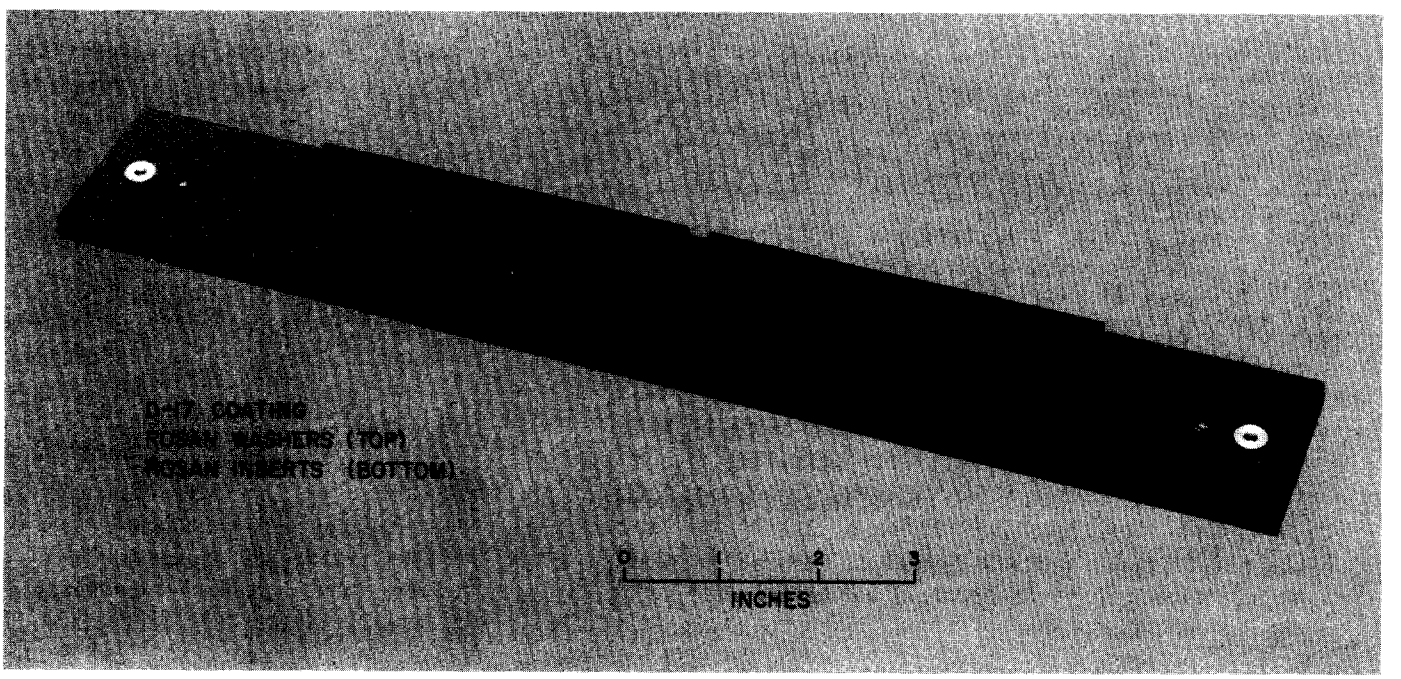

Fig. 23. Typical Dow-17 coated assembly

UNCLASSIFIED
CONFIDENTIAL

UNCLASSIFIED
CONFIDENTIAL

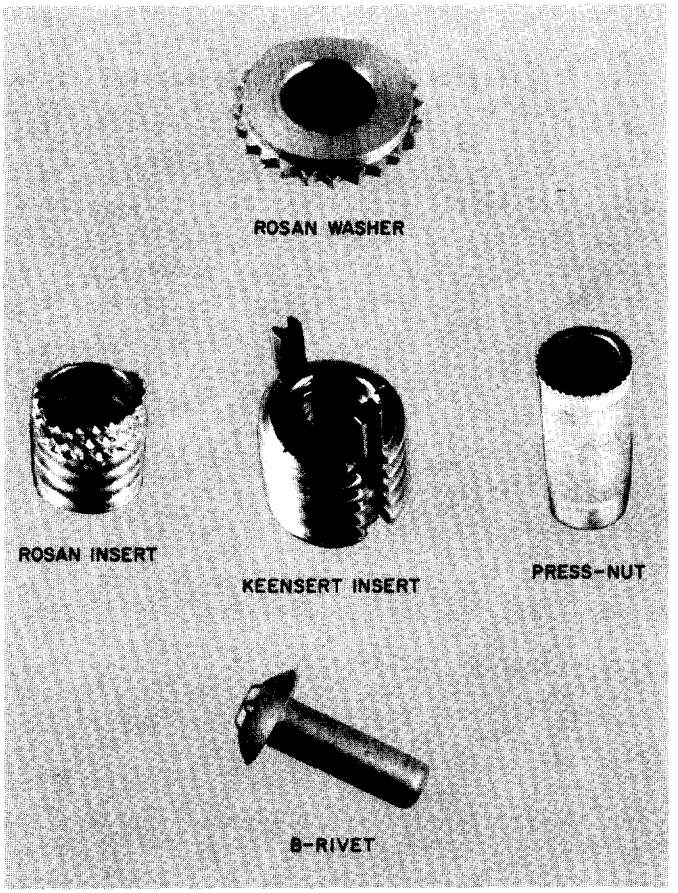

Fig. 24. Types of fasteners used to fabricate assemblies

Table 10. Resistance measurements on Dow-17 coated assemblies

Hole coating	Type of fastener		Assembly resistance, μΩ
	Top plate	Bottom plate	
Dow-17	No. 6 Rosan washer	No. 6 Keensert insert	38700
Dow-19	None	No. 6 Keensert insert	16500
Dow-17	No. 6 Rosan washer	No. 6 Rosan insert	4370
Dow-19	None	No. 6 Rosan insert	5274
Dow-19	None	No. 8 Press-nut	7265
Dow-19	None	B-rivet	4210

the Dow-17 coating operation and were then subsequently coated with Dow-19, a brush-on conversion coating.

Electrical continuity through the assemblies was determined by making resistance measurements with a double Kelvin bridge. Bare magnesium contact points were situated at each end of the assembly through which a direct current of 5 to 10 A was passed. Resistance measurements for the Dow-17 coated assemblies are presented in Table 10.

Two "control" assemblies were fabricated to correlate electrical continuity between the Dow-7 and Dow-17 coatings. These assemblies incorporated a different type of fastener at each of three joints, rather than one type of fastener throughout the entire assembly. Electrical continuity was checked by means of a double Kelvin bridge. The resistance measurements obtained on the control assemblies are presented in Table 11.

Additionally, a humidity corrosion test was conducted on the two control assemblies at 100°F and 95% relative humidity for 168 h. This test was run to check the over-all corrosion resistance of the two coatings and to determine whether corrosion occurred around the fasteners due to damage to the coatings during fastener installation. Periodic inspections were made of the assemblies for evidence of corrosion.

Discussion. Resistance measurements for the Dow-17 coated assemblies were found to be more dependent on the type of fastener and the amount of surface contact between the fastener and the magnesium plate than on the type of coating used in the fastener holes. For example, the high resistivity of the Keensert inserts conferred a correspondingly high resistance to the assembly.

In the two control assemblies, where three different types of fasteners were used in each assembly, the Dow-7 coated assembly showed a lower total resistance than did the Dow-17 coated assembly. This was probably due

Table 11. Resistance measurements on control assemblies

Surface coating	Hole coating	Type of fastener				Assembly resistance, μΩ
		Top plate	Bottom plate			
			Joint 1	Joint 2	Joint 3	
Dow-7	Dow-19	None	No. 6 Keensert insert	No. 6 Rosan insert	No. 8 Press-nut	3744
Dow-17	Dow-19	None	No. 6 Keensert insert	No. 6 Rosan insert	No. 8 Press-nut	15630

UNCLASSIFIED
CONFIDENTIAL

UNCLASSIFIED
CONFIDENTIAL

either to the conductivity of the Dow-7 coating itself or to the fact that installed fasteners of the same type exhibit a variation in resistance. However, both coated assemblies exhibited high electrical continuity.

After exposure for 24 h, the Dow-7 coated assembly showed numerous corroded areas, but no corrosion was visible on the Dow-17 coated assembly. Throughout the test the amount of corrosion increased on the Dow-7 coated assembly. Upon termination of the corrosion test, the Dow-7 coated assembly was severely corroded (Fig. 25), and no corrosion was visible on the Dow-17 coated assembly. No corrosion areas were found around the fasteners.

Conclusions. It can be concluded from this investigation that electrical continuity exists in Dow-17 coated magnesium spacecraft components joined by standard mechanical fasteners and that such coated and joined components exhibit excellent corrosion resistance.

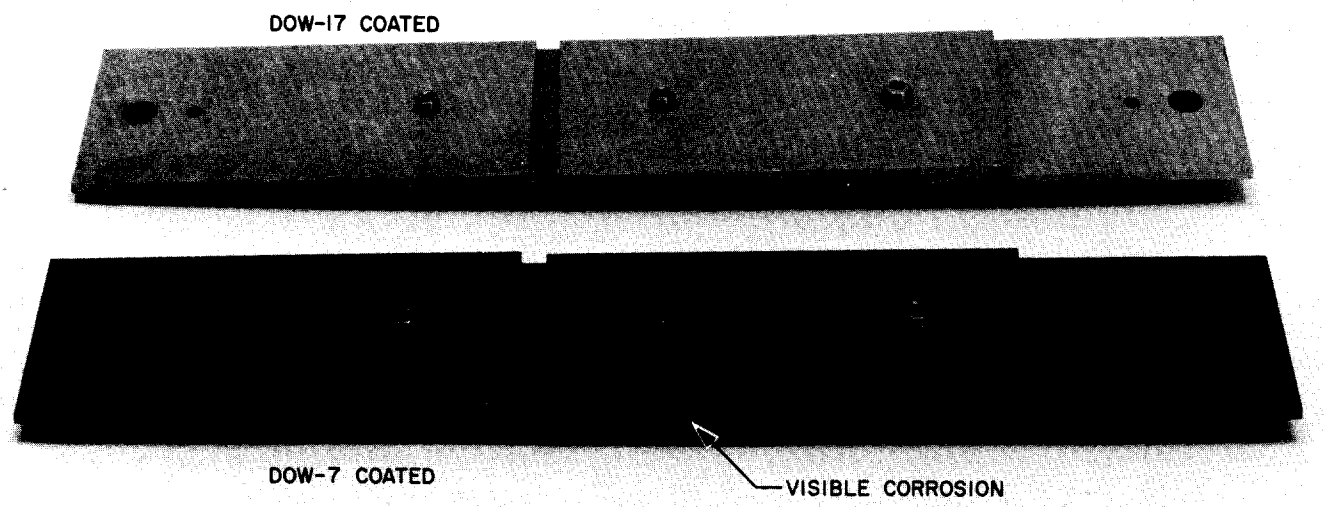

Fig. 25. Dow-7 and Dow-17 coated control assemblies after corrosion test

UNCLASSIFIED
CONFIDENTIAL

UNCLASSIFIED
CONFIDENTIAL

IV. *Voyager* Project

A. Introduction

1. Objectives

The primary objective of the *Voyager* Program is to carry out scientific investigations of the solar system by instrumented, unmanned spacecraft which will fly by, orbit, and/or land on the planets. Emphasis will be placed on acquisition of scientific information relevant to the origin and evolution of the solar system; the origin, evolution, and nature of life; and the application of this information to an understanding of terrestrial life. The primary objective of the *Voyager* missions to Mars, beginning in 1973, is to obtain information relative to the existence and nature of extraterrestrial life; the atmospheric, surface, and body characteristics of Mars and the planetary environment by performing automated experiments on the surface of, and in orbit about, the planet. A secondary objective is to further our knowledge of the interplanetary medium between the planets earth and Mars by obtaining scientific and engineering measurements while the spacecraft is in transit.

2. Project Plan

All *Voyager* missions will be conducted as events of an integrated program in which each individual flight forms a part of a logical sequence in an over-all technical plan of both lander and orbital operations. The *Voyager* design will provide for the carrying of large scientific payloads to the planet, the telemetering of a high volume of data back to earth, and long useful lifetimes in orbit about the planet and/or on the planetary surface. Hardware will be designed to accommodate a variety of spacecraft, capsule bus, and lander science payloads, mission profiles, and trajectories. Particular emphasis will be given to simple and conservative designs, redundancy wherever appropriate, and a comprehensive program of component, subsystem, and system testing.

Over-all direction and evaluation of the *Voyager* Program is the responsibility of the Office of Space Science and Applications (OSSA) of the National Aeronautics and Space Administration (NASA).

An interim project management office consisting of OSSA personnel has been established at Pasadena, California, for *Voyager* Project management, supported by the Jet Propulsion Laboratory (JPL) of the California Institute of Technology in the mission analysis and engineering area. System responsibilities assigned to JPL are: surface laboratory system, tracking and data acquisition system, and mission operations system; assigned to Marshall Space Flight Center (MSFC) are *Saturn V* launch vehicle system and spacecraft system; and to Langley Research Center (LaRC) the capsule bus system has been assigned.

UNCLASSIFIED
CONFIDENTIAL

3. Technical Description

Planning shall be based upon launching two identical planetary vehicles by a single *Saturn V* launch vehicle at each Martian opportunity, starting with the 1973 opportunity. Each planetary vehicle is to consist of a flight spacecraft, flight capsule bus, and surface laboratory, with science experiments conducted in 1973 from the orbiter, during descent and on the planetary surface. The sterilized flight capsule bus will be designed for separation from the flight spacecraft in orbit, for attaining a Mars impact trajectory, for entry into the Martian atmosphere, for descent to the surface, and for soft-landing the surface laboratory, which will have surface lifetimes of 30 days in 1973 and later goals longer than one year. The surface laboratory will contain all power, sequencing, and communications for the conduct of surface operations.

During the capsule Phase B time period, assessment shall be made of the quantitative effect of various growth factors on useful landed weight including increases in launch vehicle performance, increase in minimum Martian surface pressure, and availability of current weight contingency.

4. Sequence of Events

The Surface Laboratory System plan is being implemented as follows:

The procurement action for the total capsule system included selection of two Phase B JPL contractors May 18, 1967, and from among these, one Phase C and D LaRC contractor for the capsule bus system will be selected to carry out Phases C and D of the capsule bus system procurement. The surface laboratory Phase C procurement will be open competition for one JPL contractor who will carry out Phases C and D. The Phase C Request for Proposals is expected to be issued in December 1967.

B. Telecommunications

1. *Mariner* S-Band Turnaround Ranging Transponder Improvement Program

a. Introduction. Improvements are being made on the S-band turnaround ranging transponder used on *Mariner* Mars 1964 spacecraft so that it can be employed confidently on advanced projects. The existing circuitry is being studied by Philco's Space and Re-entry Systems Division. Selected design improvements will be incorporated in an existing *Mariner* transponder and tested in the final phase of the program. (Refer to SPS 37-42, Vol. IV, pp. 183–189, and SPS 37-43, Vol. IV, pp. 374–376, for a more detailed discussion of the transponder improvement program.)

2. Transponder Description

The S-band transponder provides the functions of a double superheterodyne command receiver, a phase-coherent transponder, a turnaround ranging transponder, and a telemetry transmitter. As shown in Fig. 1, it employs three loops: the ranging, automatic gain control (AGC), and automatic phase control (APC) loops. In the absence of a signal received from the DSIF, the spacecraft telemetry information is encoded on a signal whose frequency is controlled by an auxiliary oscillator. When a signal from the DSIF is present in the transponder receiver at a level of approximately −150 dBmW or higher, the APC loop will lock to it, and the AGC voltage will develop in the AGC loop. This voltage, besides controlling the receiver gain for proper operation, also produces a command voltage which turns off the auxiliary oscillator and causes the 19.125-MHz voltage-controlled oscillator to be switched to the transmitter input in its place. In this manner, closing the APC loop provides an exact ratio of 240 to 221 between the transmitted and received frequencies. In addition, the AGC voltage is telemetered to provide received signal strength information.

The signal received from the DSIF may have either range or command information phase modulated on it. The second mixer provides two outputs, one to the 9.56-MHz narrow-band command and APC channel, and another to the broad-band 9.56-MHz range channel. The range code is demodulated by the phase detector in the range channel, amplified, and remodulated onto the transmitted signal along with the telemetry input. The command information is demodulated by the phase detector in the narrow-band channel.

Physically, the transponder consists of 13 modules, which correspond to the blocks in Fig. 1. These modules are grouped together in "six-packs," two six-packs for the receiver, and one six-pack for two (redundant) transmitters. The complete transponder weighs approximately 10½ lb.

3. Design Problems

Because of the tight *Mariner* Mars 1964 schedule, some design problems, such as those encountered in the S-band transponder, were allowed to remain. The transponder

UNCLASSIFIED
CONFIDENTIAL

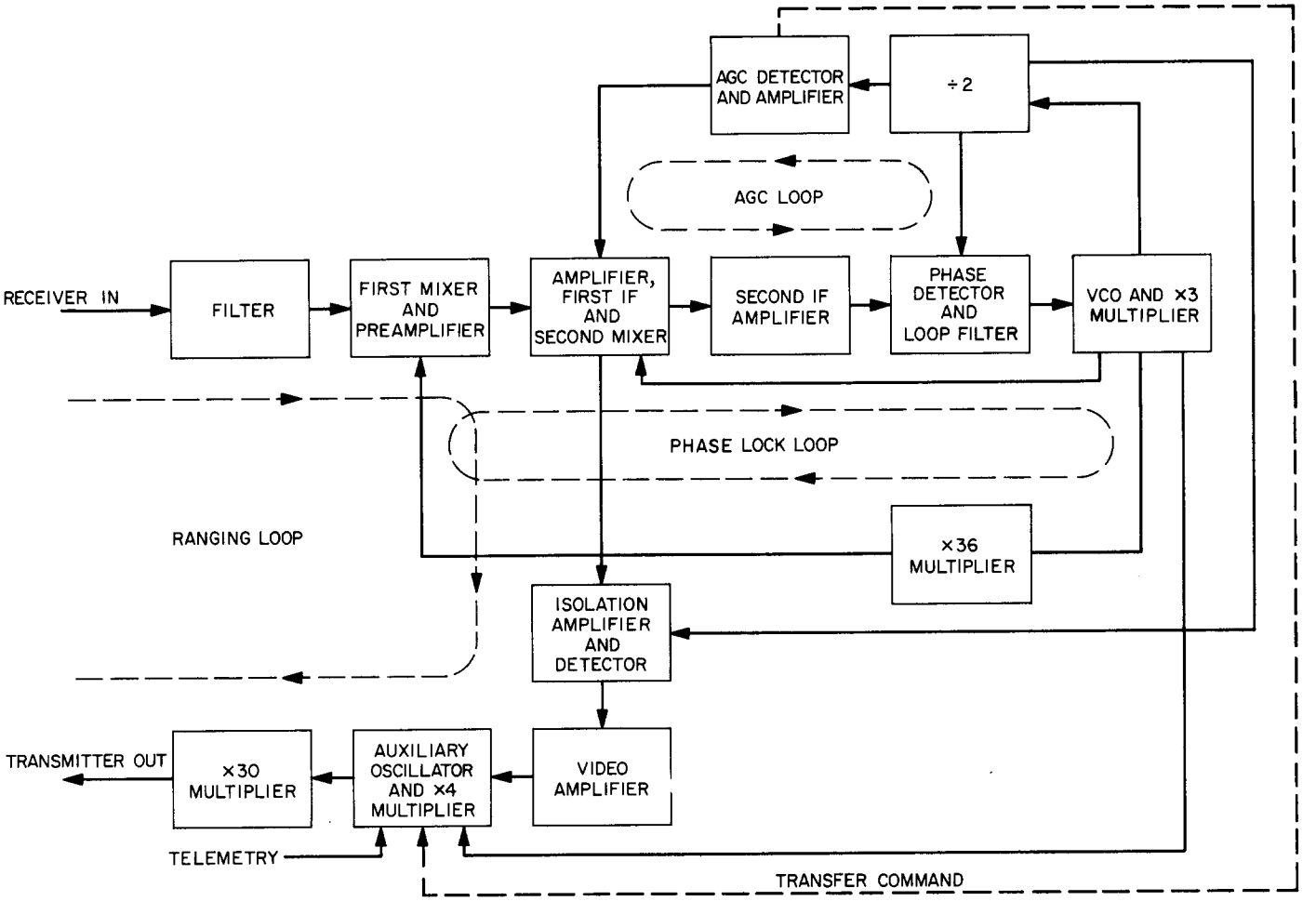

Fig. 1. S-band ranging transponder block diagram

problems were of two types: system problems and problems peculiar to individual modules.

Three main system problems were found to exist. Under certain conditions, the transponder APC loop would lock to a transponder-generated signal when the range channel was turned on, and this prevented the reception of the ground station signal. The turnaround delay time for the ranging modulation varied excessively with temperature, which prevented accurate range determination. The transponder AGC voltage versus received signal strength characteristic varied excessively with temperature. This reduced the accuracy with which received signal strength could be determined.

Module performance parameters were unstable with temperature and voltage fluctuations; the modules were not readily reproducible, and tests and adjustments were long and tedious.

4. Analysis and Experimental Work

The transponder improvement study consists of both analysis and experimental work. Ranging and AGC performance and the self-lock phenomenon have been analyzed, and ranging delay variation measurements are being performed. Improved versions of the first and second IF amplifiers and the ×30 multiplier have been completely breadboarded. Partial breadboards have been built of improved versions of the mixer–preamplifier, AGC detector, VCO, and auxiliary oscillator. Some recommendations have been made, and improvements are being made on the phase detector, frequency divider, and ×36 multiplier in the *Mariner* Mars 1969 transponder.

a. Self-lock. To produce self-lock, a spurious output signal must be generated by the transponder transmitter, and a receiver response must exist near the spurious signal frequency. Then if the ranging channel is turned on, modulating the transmitter, the receiver locks onto the

CONFIDENTIAL
UNCLASSIFIED

spurious signal. This spurious signal may be generated anywhere in the ranging loop. One source is a spurious oscillation in the ×30 multiplier, produced by mismatching its output. At certain phase angles, mismatches as low as 1.2 can cause spurious outputs.

A breadboard of a redesigned ×30 multiplier was built and tested, using a transistor amplifier–multiplier instead of a varactor. The breadboard is substantially less subject to the effects of impedance mismatch than the original design, and it showed no spurious output with impedance mismatches as high as 2, at any phase angle.

Another possible cause of self-lock is leakage of coherent signals between modules. Improvements are being made in interstage and intermodule filtering and shielding to increase the margin of safe operation against this mode of self-lock.

b. Ranging. The ranging improvements are directed toward reducing the turnaround ranging time delay variations through the transponder and increasing the ranging modulation bandwidth. Increasing the bandwidth will help reduce time delay variations.

The time delay through the *Mariner* transponder varies with temperature by as much as 200 ns, or 30 m round trip range. The DSIF specifies a maximum variation of 100 ns, but would prefer substantially less. Preliminary calculations were made of the absolute delay of each module due to bandwidth and transistor transit times. The effects of temperature and signal level variations on the turnaround ranging delay time of the transponder were measured. Delay measurements are being made with each module individually subjected to temperature testing in order to evaluate and isolate the causes of the variation. Measurements will be made of doppler delay variations through the transponder at S-band.

Breadboard modulator and ×30 multiplier circuits were built and tested with a resulting increase in modulation bandwidth from a marginal 1.8 to more than 4 MHz and a decrease in the effects of temperature on modulator sensitivity from ±10 to ±5%.

To reduce the ×5 multiplier stage effect on the high-frequency modulation response of the range channel, a different multiplier order is being investigated. The ×5 stage in the ×30 multiplier will be interchanged with the ×4 stage in the auxiliary oscillator. Tests will be made of the modulation performance of improved breadboards incorporating this change.

A new auxiliary oscillator was designed. Closer tolerances were put on the crystal temperature coefficient and a less temperature-sensitive oscillator circuit was produced. These changes resulted in a substantial reduction in auxiliary oscillator drift.

The video amplifier will be redesigned to broaden its response, improve its rejection of spurious signals, and improve its limiting action so that the ranging modulation index will be more constant with variations in uplink signal.

c. Automatic gain control. Excessive over-all drift of the AGC loop characteristics occurred because of drifting of the dc amplifier and detector output, and gain variations in the IF amplifiers, with temperature and power supply voltage variations. The dc amplifier was extremely sensitive to temperature variations, particularly at high temperatures where drift of the output reached as much as 3 V.

A commercial operational amplifier has been suggested as a possible replacement for the dc amplifier and is being evaluated. The detector output drift appears to be due to the inherent characteristics of its parts. The drift consists mainly of diode drift, with a minor contribution from phase error. Temperature compensation of the diodes will be investigated. The 47.8-MHz IF amplifier was redesigned to use four grounded emitter signal transistor amplifier stages instead of the original three cascode amplifiers. Linearity was improved approximately 3 to 1, and temperature drift was reduced to less than 4 dB. Redesign of the 9.56-MHz IF linear amplifier reduced the gain drift with temperature to <1 dB. Differential phase shift variations between limited and linear outputs with temperature were reduced from 45 to 2.5 deg. Output linearity was improved from a ±2- to ±0.5-dB departure from a straight line.

d. Transponder threshold. A 1-dB improvement in transponder threshold performance under worst-case conditions (high temperature and low drive) was accomplished by redesigning the first mixer in the mixer–preamplifier to use hot carrier mixer diodes and by changing to a lower noise transistor in the first stage of the IF amplifier following the mixer. The input voltage standing-wave ratio of the new mixer–preamplifier was reduced from 1.8:1 to 1.5:1, and the output impedance was stabilized at 50 Ω.

UNCLASSIFIED
CONFIDENTIAL

V. Future Projects

The Future Projects Office of the Laboratory is responsible for the direction, sponsorship and, in cooperation with other elements of the Laboratory, the origination of advanced mission and future project studies in the areas of interest and applicability to the Laboratory.

The objective of this effort is to insure that the preliminary technical information and plans for the various potential missions, together with the associated information on spacecraft systems, instrumentation systems, launching vehicle systems, resources, and schedules be available as required. This preliminary mission study information will be used primarily for defining specific flight mission programs and as generalized guidance for Laboratory research and advanced development programs.

Each study conducted by this Future Projects Office has been, and will continue to be, documented in a formal final report. This section of the Space Programs Summary is allocated to provide an abstract or summary of the results of each study including, where appropriate, reference to the final report for additional details.

CONFIDENTIAL
UNCLASSIFIED